



<https://doi.org/10.11646/phytotaxa.479.1.1>

Three new needle-shaped *Fragilaria* species from Central America and the Tibetan Plateau

KIM J. KRAHN^{1,7*}, ANJA SCHWARZ^{1,8}, CARLOS E. WETZEL^{2,9}, SERGIO COHUO-DURÁN^{1,3,10}, GERHARD DAUT^{4,11}, LAURA MACARIO-GONZÁLEZ^{1,5,12}, LISETH PÉREZ^{1,13}, JUNBO WANG^{6,14} & ANTJE SCHWALB^{1,15}

¹ Technische Universität Braunschweig, Institute of Geosystems and Bioindication, Langer Kamp 19c, 38106 Braunschweig, Germany.

² Luxembourg Institute of Science and Technology (LIST), Environmental Research and Innovation Department (ERIN), 41 rue du Brill, 4422 Belvaux, Luxembourg.

³ Tecnológico Nacional de México – I. T. Chetumal., Av. Insurgentes 330, Chetumal, 77013 Quintana Roo, Mexico.

⁴ Friedrich-Schiller-University Jena, Institute of Geography, 07743 Jena, Germany.

⁵ Tecnológico Nacional de México – I. T. de la Zona Maya, Carretera Chetumal-Escárcega Km 21.5, Ejido Juan Sarabia, 77965 Quintana Roo, Mexico.

⁶ Key Laboratory of Tibetan Environment Changes and Land Surface Processes (TEL) / Nam Co Observation and Research Station (NAMORS), Institute of Tibetan Plateau Research, Chinese Academy of Sciences, Beijing 100101, China.

⁷ [✉ k.krahn@tu-bs.de](mailto:k.krahn@tu-bs.de); <http://orcid.org/0000-0002-1646-7612>

⁸ [✉ anja.schwarz@tu-braunschweig.de](mailto:anja.schwarz@tu-braunschweig.de); <http://orcid.org/0000-0003-0722-2354>

⁹ [✉ carlos.wetzel@list.lu](mailto:carlos.wetzel@list.lu); <http://orcid.org/0000-0001-5330-0494>

¹⁰ [✉ Sergiocd@comunidad.unam.mx](mailto:Sergiocd@comunidad.unam.mx); <http://orcid.org/0000-0002-7514-2084>

¹¹ [✉ gerhard.daut@uni-jena.de](mailto:gerhard.daut@uni-jena.de); <http://orcid.org/0000-0001-7414-1103>

¹² [✉ lauramg133@hotmail.com](mailto:lauramg133@hotmail.com); <http://orcid.org/0000-0002-6105-8033>

¹³ [✉ l.perez@tu-braunschweig.de](mailto:l.perez@tu-braunschweig.de); <http://orcid.org/0000-0002-5256-3070>

¹⁴ [✉ wangjb@itpcas.ac.cn](mailto:wangjb@itpcas.ac.cn); <http://orcid.org/0000-0003-2335-519X>

¹⁵ [✉ antje.schwalb@tu-braunschweig.de](mailto:antje.schwalb@tu-braunschweig.de); <http://orcid.org/0000-0002-4628-1958>

*Author for correspondence: [✉ k.krahn@tu-bs.de](mailto:k.krahn@tu-bs.de)

Abstract

Three new needle-shaped *Fragilaria* species from freshwater lake Apastepeque in El Salvador (*Fragilaria salvadoriana* sp. nov., *F. maarensis* sp. nov.) and subsaline lake Nam Co on the Tibetan Plateau (*F. huebeneri* sp. nov.) are described and compared based on light and scanning electron microscopy observations and morphometric analyses. *Fragilaria salvadoriana* sp. nov. is characterized by narrowly linear-lanceolate, sometimes centrally constricted valves, subcapitate to rarely capitate apices, and a distinct, dented appearing central area. Striae are composed of 2–5 occluded areolae. It can be differentiated from similar needle-shaped species by the valve outline, relatively low striae density, and shark fin-shaped spines. Characteristic of *F. maarensis* sp. nov. are a very narrowly lanceolate valve outline and subcapitate apices. The apical pore field is composed of 2–3 rows of poroids and acute, irregularly oriented spines are present at the junction between valve face and mantle. This taxon is clearly different from other *Fragilaria* species, displaying a high length-to-width ratio and a low number of areolae per stria. The Tibetan species, *F. huebeneri* sp. nov., forms long ribbon-like colonies linked together by spatula-shaped spines. Valves have subcapitate apices, a spindle- to needle-shaped outline and an indistinct central area. Striae are alternate and composed of 3–5 areolae per stria. Teratological forms of *F. huebeneri* sp. nov. were commonly observed in the sediment trap samples. *Fragilaria salvadoriana* sp. nov. and *F. maarensis* sp. nov. were found in a warm, tropical crater lake characterized by low conductivity and dissolved oxygen content, medium alkaline pH, and magnesium-calcium-bicarbonate-rich waters. *Fragilaria huebeneri* sp. nov. was frequent in a large, high elevation lake with increased specific conductivity, alkaline pH and sodium-bicarbonate-rich waters. The new species are compared to morphologically similar species from the genus *Fragilaria* Lyngbye and ecological preferences are discussed.

Keywords: Bacillariophyceae, diatoms, China, El Salvador, freshwater, Neotropics, subsaline, taxonomy

Introduction

The concept of the genus *Fragilaria* Lyngbye (1819: 182) is not well defined in the original description by Lyngbye (1819) and encompasses species that form linear colonies. A revision by Williams & Round (1987) resulted in the

narrower genus concept of *Fragilaria* *sensu stricto*. Several characters such as open girdle bands, apical pore fields of the ocellulimbus-type, a single rimoportula per valve at the apex, presence of spines, and uniserial striae are presented. However, species without spines and with two rimoportulae per valve were recently also ascribed to the genus *Fragilaria* (e.g. Almeida *et al.* 2016). Round *et al.* (1990) stated that *Fragilaria* species are restricted to freshwater habitats, although some species from habitats with increased salinities have been reported (Witkowski *et al.* 2000, Rioual *et al.* 2017).

Needle-shaped *Fragilaria* species are often abundant in the plankton of different types of freshwater lakes and commonly observed during biomonitoring (Lange-Bertalot & Ulrich 2014; Rühland *et al.* 2015; Almeida *et al.* 2016; Kahlert *et al.* 2019). Nonetheless, the specific characteristics which are important for distinguishing the diatom genus *Fragilaria* from related genera and their individual relevance are still under discussion (e.g. Williams & Round 1986, 1987, Williams 2011, Rioual *et al.* 2017, Williams 2019). Many species belonging to *Fragilaria* have been described from Europe and North America (e.g. Patrick & Reimer 1966, Morales 2003, Lange-Bertalot & Ulrich 2014). Especially scanning electron microscopy (SEM) and molecular analyses have resulted in a large number of new species and separate genera (Williams & Round 1987, Medlin *et al.* 2008, Lange-Bertalot & Ulrich 2014, Kahlert *et al.* 2019).

In general, overall biological diversity is believed to increase from northern latitudes to the equator line (Mittelbach *et al.* 2007), and remote regions also potentially harbor species new to science. However, there is little floristic information on diatoms available for Central America (e.g. Hustedt 1953, Michels-Estrada 2003, Castillejo *et al.* 2018) and the Tibetan Plateau (e.g. Zhu & Chen 1995, 1996). Due to difficulties in identifying morphological characters in light microscopy (LM), species have often been “force-fitted” into existing concepts (Morales *et al.* 2014).

Studies investigating the present-day distribution and ecology of diatoms in different regions of Central America are mostly from Costa Rica. Water quality assessments of Costa Rican rivers in particular have involved diatoms and associated physico-chemical parameters being documented and analyzed. The results demonstrate a strong correlation of several species with certain environmental variables (e.g. pH, conductivity) and thereby the high indicator qualities of diatoms (Silva-Benavides 1996a, b, Michels 1998a, b, Michels *et al.* 2006, Céspedes-Vargas *et al.* 2016, Flores-Stulzer *et al.* 2017). Wydrzycka & Lange-Bertalot (2001) contributed to the knowledge of acidophilic diatoms in Costa Rica by recording diatoms from nine sites connected to the extremely acid Agrio River with varying pH. Moreover, a study of 25 lakes indicated cation concentrations and lake area and depth to be important drivers of diatom distribution in Costa Rica (Haberyan *et al.* 1997). Pérez *et al.* (2013) analyzed surface sediments from 63 waterbodies located from NW Yucatán Peninsula (Mexico) to southern Guatemala. The samples were distributed along a broad gradient of trophic state, altitude, and precipitation, and results determined conductivity as the main variable influencing distribution pattern of diatoms in this region. Furthermore, taxonomic studies describing new species were recently published from e.g. Panama (Lange-Bertalot & Metzeltin 2009), El Salvador (Wetzel & Ector 2014, Krahn *et al.* 2018) and Guatemala (Paillès *et al.* 2018).

On the Tibetan Plateau, studies investigating the recent distribution patterns of diatoms in lakes identified water depth and salinity as the two most important environmental variables (e.g. Yang *et al.* 2001, 2003, Yu *et al.* 2019). Furthermore, the number of publications using diatoms for paleoenvironmental reconstructions, for example to infer Holocene climatic and hydrological changes in western Tibet (Van Campo & Gasse 1993, Gasse *et al.* 1996), is steadily increasing. Taxonomical studies reach far back (Mereschkowsky 1906, Hustedt 1922; Skvortzow 1935; Jao 1964; Jao *et al.* 1974; Huang 1979; Li 1983) and several new species (e.g. Chudaev *et al.* 2016, Liu *et al.* 2018, 2019) and even one genus (*Tibetiella* Y.L.Li, D.M.Williams & Metzeltin 2010) endemic to China (Li *et al.* 2010) have recently been described. Skvortzow (1935) described *Fragilaria curvata* Skvortzow 1935 from a small river arising from the base of Tibet. Moreover, the type material of *Fragilaria asiatica* Hustedt (1922: 119), collected in 1900 in Tibet, was reanalyzed and SEM images yielded new insights into the morphological characteristics of this species (Rioual *et al.* 2017). Nonetheless, studies dealing with the genus *Fragilaria* from this area are still scarce. Kocolek *et al.* (2020) recently compiled an inventory of continental diatom taxa described from inland waters in China.

The purpose of this study is to expand knowledge of the morphology and ecology of needle-shaped *Fragilaria* species occurring in freshwater and subsaline lakes. We present a detailed description of three new species from El Salvador and the Tibetan Plateau and provide a comparison with similar taxa.

Material and methods

Study areas and collection of samples and water parameters

El Salvador is characterized by a diverse physiography, a tropical climate with little temperature variation throughout

the year, and pronounced rainfall seasonality (average rainfall ~1861 mm/yr). The rainy season, often accompanied by heavy rainfall, extends from May to October, while dry conditions prevail from November to April (Sayre & Taylor 1951, MARN 2015, Armenteras *et al.* 2016). The average yearly temperature is about 23.8 °C (MARN 2015).



FIGURE 1. Map of Central America (upper right square) and El Salvador with location of Lake Apastepeque (black dot).

The Apastepeque Volcanic Field, situated in the department of San Vicente in central El Salvador, is a relatively young volcanic area composed of a densely spaced complex of cinder cones, lava domes, and maars (Williams & Meyer-Abich 1955, Meyer-Abich & Williams 1956). Lake Apastepeque ($13^{\circ}41'32.84''N$ and $88^{\circ}44'42.41''W$, Fig. 1) is a small (~0.35 km²), almost circular volcanic lake, displaying a maximum depth of 54 m. It is located at an elevation of 504 m a.s.l. (Jiménez *et al.* 2004). In October 2013, a ~30 cm long sediment core and surface sediments (0–1 cm) were retrieved from 47 m water depth using a Uwitec gravity corer and Ekman grab, respectively. Physicochemical parameters of the surface water (at 0.5 m) were measured during sample collection with a WTW Multi Set 350i multiparameter probe, and water transparency was determined using a Secchi disk (Table 1). To determine the lake waters ionic dominance, ion concentrations were transformed to meq/L. Field measurements suggest a warm monomictic lake with anoxic bottom conditions. Studies from Mexico show that many small, deep crater lakes can be ascribed to this type (Alcocer *et al.* 2000, Vázquez *et al.* 2004). However, more data is needed for verification.

TABLE 1. *In-situ* limnological measurements and water chemistry data from surface waters of Lake Apastepeque (AP) and Nam Co (NC). AP: data from October 2013. NC (station T2): limnological measurements (May to September 2012), water chemistry data (May 2012), SD (June 2012, Wang *et al.* 2019). Abbreviations and units: T=Surface water temperature [°C], DO=Dissolved oxygen [mg/L], Cond=Electrical conductivity [μS/cm], Sal=Salinity [%], SD=Secchi depth [m], Major ions [mg/L].

	T	DO	pH	Cond	Sal	SD	HCO ₃ ⁻	HCO ₃ ⁻ +CO ₃ ²⁻	SO ₄ ²⁻	Cl ⁻	Na ⁺	K ⁺	Ca ²⁺	Mg ²⁺
AP	29.5	2.8	8.6	100	0	6.1	145.2	-	7.6	10.5	10.8	7.5	17.9	15.2
NC	3.3–11.8	5.6–7.1	9.4–9.9	1,716–1,851	0.9–1.0	18.0	-	1,111	192.6	59.9	323.7	38.0	13.3	103.4

Nam Co (Fig. 2, Table 1), located on the central Tibetan Plateau (TP) ($30^{\circ}40'00.0''\text{N}$, $90^{\circ}30'00.0''\text{E}$), is the third largest lake on the TP. It covers an area of around $2,026 \text{ km}^2$ and is up to $\sim 100 \text{ m}$ deep (Wang *et al.* 2009, Zhang *et al.* 2014, Wang *et al.* 2020). The dimictic, endorheic lake is completely ice-covered from late January to mid-late April (Gou *et al.* 2017, Wang *et al.* 2019, 2020). Minimum air temperatures occur in February, while July is the warmest month (-10.2°C and 9.2°C , respectively). The region is influenced by the monsoon with increased precipitation between May and October and a total precipitation of an average 457 mm/yr (Lazhu *et al.* 2016). Its climatic sensitivity makes the study area highly interesting for investigating environmental changes on the TP (Schwab *et al.* 2008, Anslan *et al.* 2020).

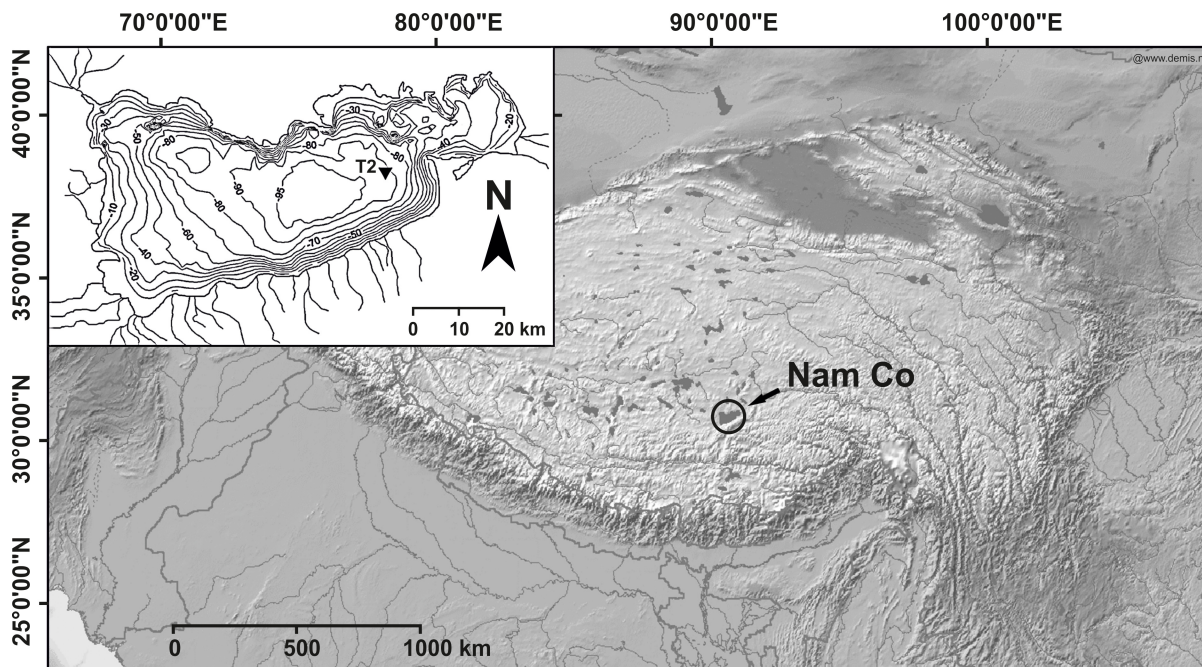


FIGURE 2. Location of Nam Co (circle) on the Tibetan Plateau and bathymetric map of the lake (upper left square) with position of station T2 (triangle).

From May to September 2012 and November 2012 to May 2013, integral sediment traps (Bloesch & Burns 2006) were installed in the deep main basin of Nam Co (station T2, $\sim 93 \text{ m}$ water depth) to determine the phytoplankton structure at different water depths. Furthermore, sequential sediment traps monitored the seasonal phytoplankton succession from June to November 2012 in 14-day resolution. Concurrently, regular water quality and temperature profiling were conducted at the mooring station. More detailed information can be found in Kai *et al.* (2020).

Sample preparation and analysis

The sediment core from Lake Apastepeque was cut into 2 cm thick section for analysis. Diatom samples from this sediment core (APA_2013) and the integral sediment trap (station T2, 30 m , May to September 2012) of Nam Co were cleaned by adding concentrated hydrochloric acid (37%) and hydrogen peroxide (30%), and heating to 70°C to remove carbonates and to oxidize organic matter, respectively (adapted from Battarbee *et al.* 2001). Subsequently, samples were centrifuged and washed with distilled water five to six times during preparation to dilute acid and oxidant remnants. Naphrax® solution was used as a mountant to prepare permanent slides for LM analyses.

Diatom slides were analyzed using a Leica DM 5000 B LM equipped with a ProgRes® CT5 camera with Differential Interference Contrast under oil immersion at $\times 1000$ magnification. Cleaned samples for SEM were filtered through a $3 \mu\text{m}$ pore diameter polycarbonate membrane, put on adhesive carbon tabs, and fixed on aluminum pin stubs. Stubs were sputter-coated with platinum using a BAL-TEC MED 020 Modular High Vacuum Coating System for 30 s at 100 mA and investigated using an ultra-high-resolution analytical field emission (FE) SEM Hitachi SU-70 (Hitachi High-Technologies Corporation, Tokyo, Japan).

Samples with high abundances of the new taxa were selected for description of the three *Fragilaria* species. Measurements of each species were taken from 35 valves of the designated holotype samples (Lake Apastepeque: APA_D_28–30cm; Nam Co: T2G2nd_30m) and for species from El Salvador additionally from sample APA_D_20–22cm. Plates displaying light and scanning electron microscopy images were created using CorelDRAW Graphics Suite 2018®. Morphometric analysis is based on measurements for species description in LM. Boxplots of the morphometric

parameters valve length, valve width, stria density, and length-to-width ratio were prepared using the program PAST (Hammer *et al.* 2001) to visualize similarities and differences between the three species. Additionally, a Hotelling's multivariate discriminant analysis (Hotelling 1951), including a paired sample Hotelling's T-square test, was performed to test morphometric differences (length, width, stria density, and length/width ratio) between species. Holotype slides of the three species were deposited in the Meise Botanic Garden, Belgium.

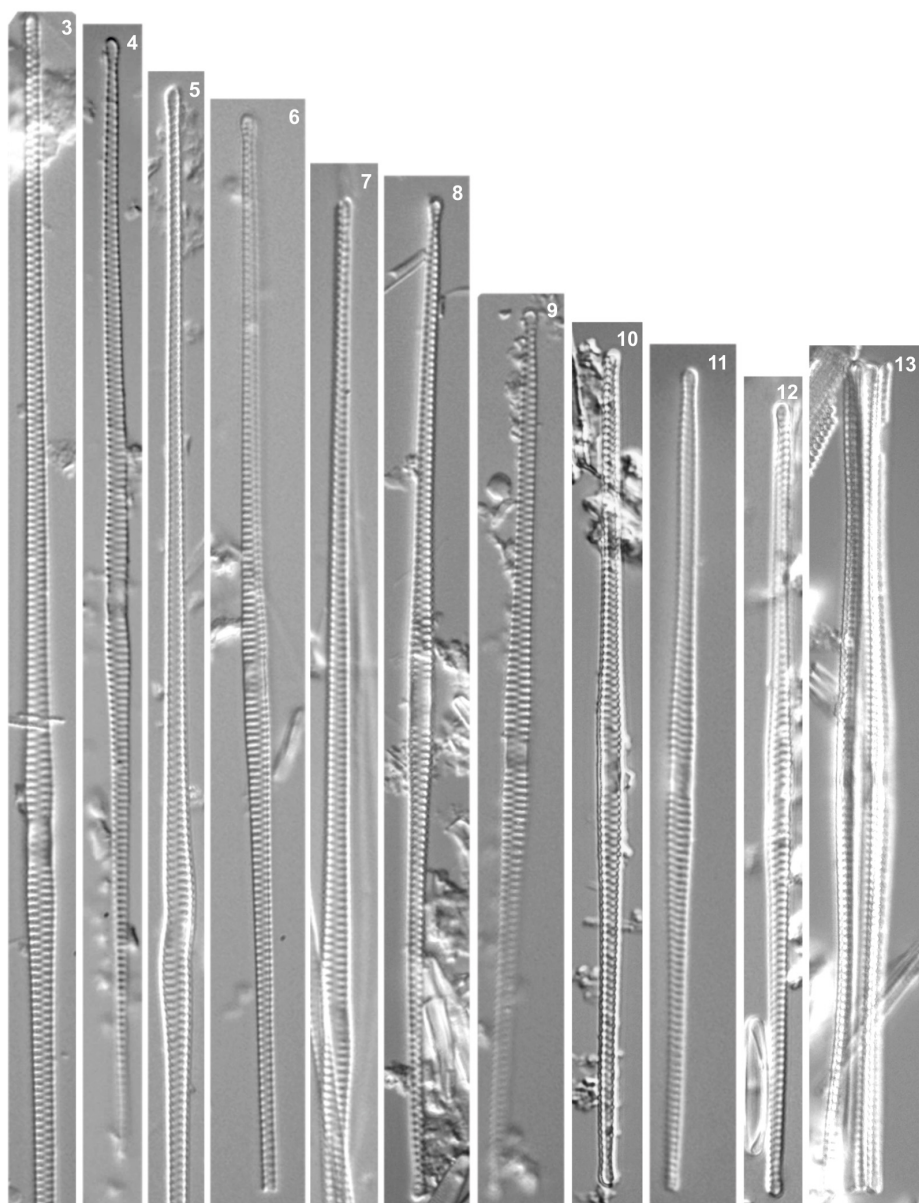
Results

Fragilaria salvadoriana K.J.Krahn et C.E.Wetzel sp. nov.

(Figs 3–13 (LM), 14–23 (SEM))

Light microscope observations

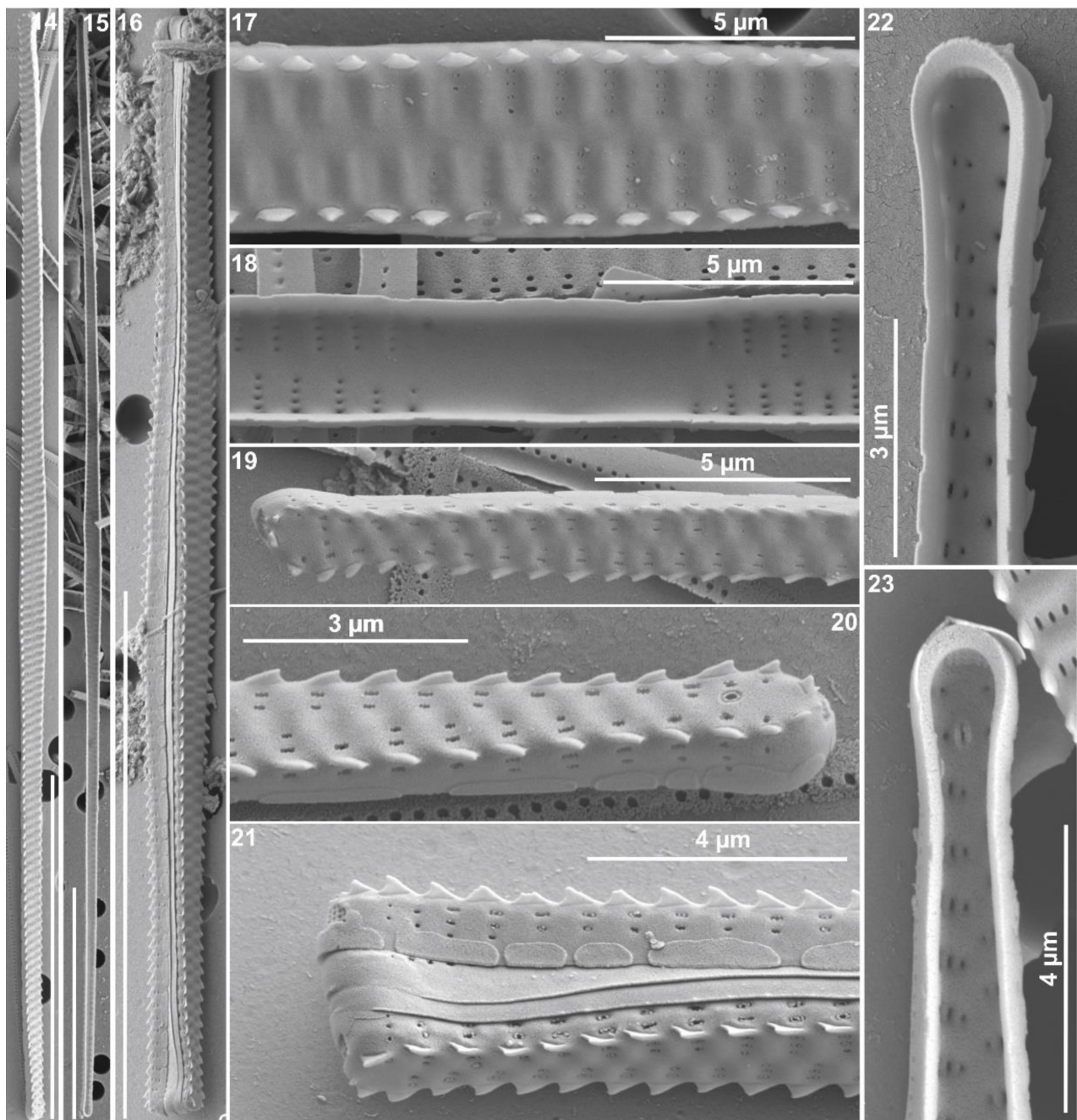
Valves narrowly linear-lanceolate, slightly narrowing towards subcapitate to slightly capitate apices (Figs 3–13). Central area distinct in LM, often appearing dented and slightly constricted with ghost striae present. Axial area narrow. Length 66–168 µm, width 2.3–3.1 µm, becoming 1.0–1.5 µm subapically and 1.3–1.7 µm at the apices (n=35). Length-to-width ratio 24–65. Alternate striae, 13.3–14.5 in 10 µm.



FIGURES 3–13. *Fragilaria salvadoriana* sp. nov., LM. Figs 3–12. Valve views. Fig. 13. Girdle view. Scale bar = 10 µm.

Scanning electron microscope observations

Striae proximally composed of 2–5 areolae on valve face and 2–4 areolae on mantle (Figs 16, 17). Areolae rounded to slightly elongated and covered by disc-like vela (Figs 17, 21). Central area is formed by absent and shortened striae (Fig. 17). Marginal, shark fin-shaped spines located throughout entire valve at junction between valve face/mantle (Figs 14, 16, 17, 19–21). Spines generally located on vimines, reaching onto virgae (Figs 17, 21). Small, acute apical spines present at apices (Figs 19–21). Apical pore fields of the ocellulimbus-type with 2–4, rarely 5 rows of poroids (Figs 19–23). One rimoportula is present per valve positioned at a distal end (Figs 20, 23). Central area is formed by absent and shortened striae (Fig. 17). Girdle bands open with small poroids on the copulae and silica plaques often present on the mantle (Figs 16, 20, 21).



FIGURES 14–23. *Fragilaria salvadorensis* sp. nov., SEM. 14. Valve in external view displaying the striae and areolae structure. 15. Valve in internal view. 16. Entire frustule showing open girdle bands and ornamentation. 17. External view of central area with ghost striae. 18. Internal view of central area. 19. External view of apex without rimoportula. Small apical spines present. Apical pore field of ocellulimbus-type. 20. External view of apex with rimoportula. 21. Girdle view of an apex showing disc-like covered areolae, shark fin-shaped spines and plaques on the mantle. 22. Internal view of apex without rimoportula. 23. Internal view of apex with rimoportula. Scale bar = 30 µm in Figs 14–16.

Type locality:—EL SALVADOR. Department of San Vicente: Lake Apastepeque, volcanic crater lake, 509 m a.s.l., 13°41'32.84"N, 88°44'42.41"W, sediment core sample (APA_D_28–30cm), 47 m water depth, collection: L. Macario-González and S. Cohuo-Durán, 09.10.2013. Holotype BR!: slide BR-4588 (Meise Botanic Garden, Belgium).

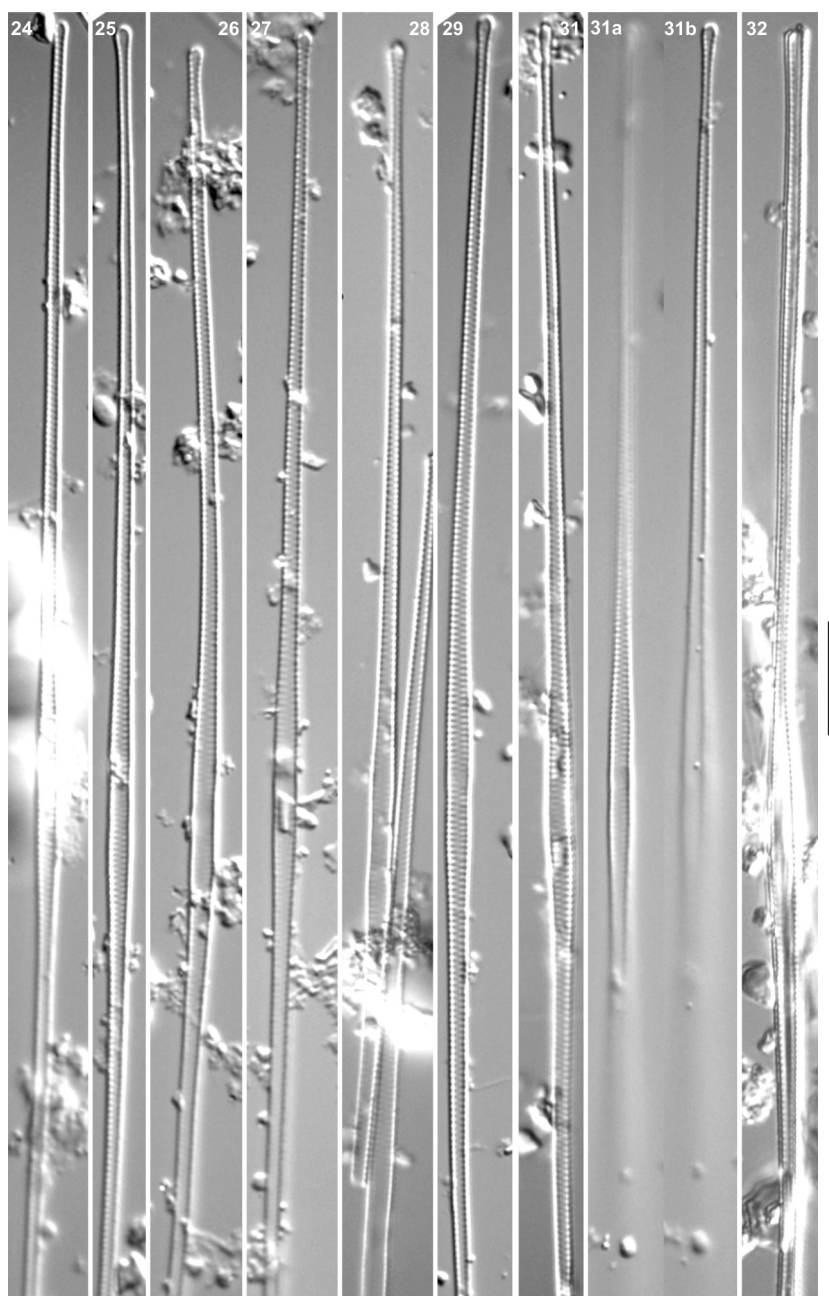
Etymology:—The specific epithet refers to the country where the new species was found: El Salvador.

***Fragilaria maarensis* K.J.Krahn et C.E.Wetzel sp. nov.**

(Figs 24–32 (LM), 33–42 (SEM))

Light microscope observations

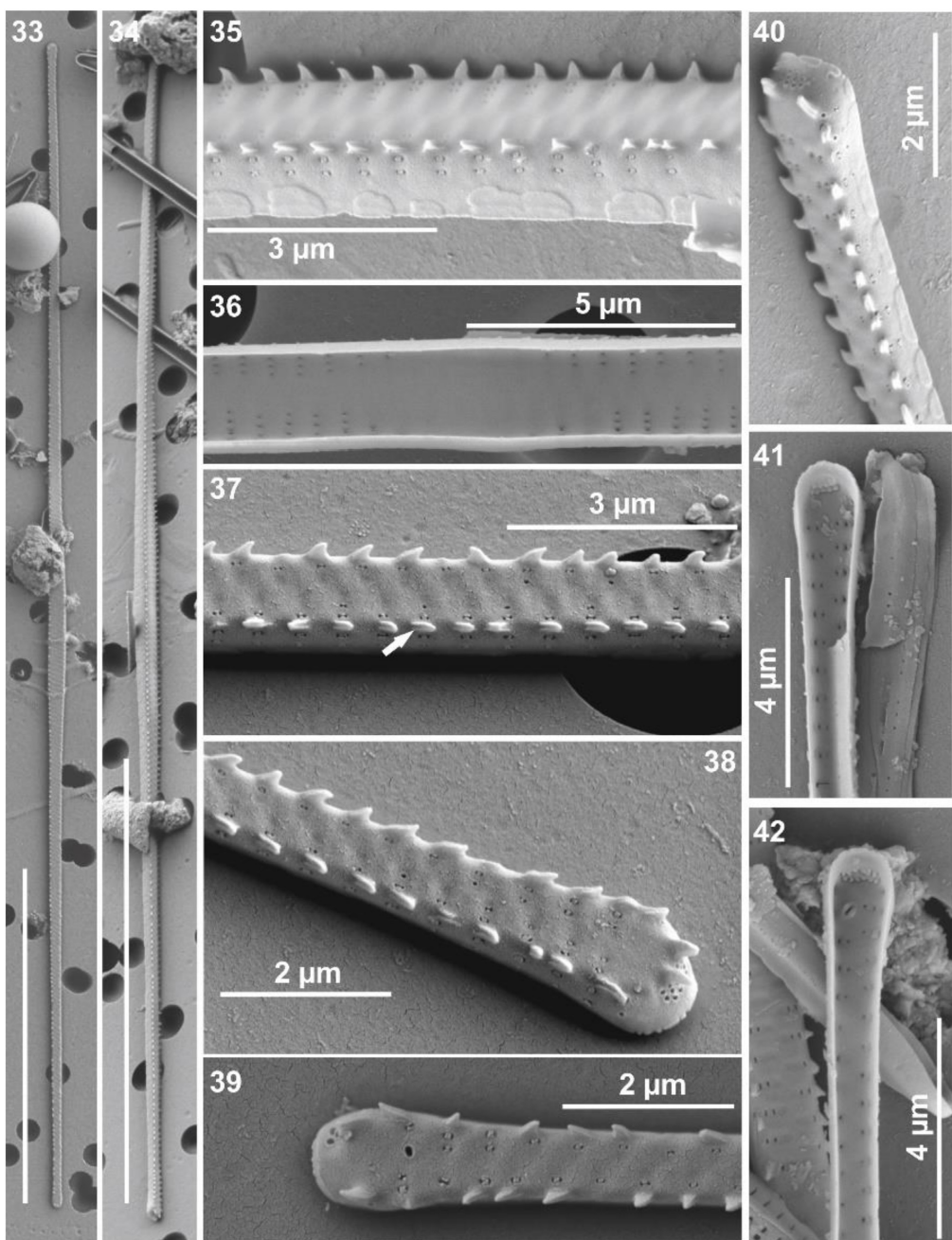
Valves very narrowly lanceolate, slightly tapering towards the subcapitate apices (Figs 24–32). Central area marked by ghost striae. Axial area narrow to narrowly lanceolate. Length 119–141 µm, width 1.8–2.6 µm, becoming 0.7–1.3 µm subapically and 1.0–1.7 µm at the apices (n=35). Length-to-width ratio 50–76. Alternate striae, 17.5–20.5 in 10 µm.



FIGURES 24–32. *Fragilaria maarensis* sp. nov., LM. Figs 24–31. Valve views. Fig. 32. Girdle view. Scale bar = 10 µm.

Scanning electron microscope observations

Striae proximally composed of 2–3, rarely 4 areolae on valve face and 2–3 areolae on mantle (Figs 35, 36). Areolae mostly rounded, sometimes slightly elongated, and covered by disc-like vela (Figs 35, 37–42). Central area is formed by absent and shortened striae (Fig. 35). Plaques often observed on the mantle (Figs 35, 40). Marginal spines irregularly orientated and located throughout entire valve at junction between valve face/mantle except for some reduced spines (Figs 33, 34, 35, 37–40). Spines are acute, bear a fine groove at the site and are generally located on the vimines (Fig. 37). Acute spines present at apices (Figs 38–40). Apical pore fields of the ocellulimbus-type with 2–3 rows of poroids (Figs 38, 40–42), sometimes reduced (Fig. 39). One rimoportula is present per valve positioned at a distal end (Figs 39, 42). Open girdle bands with small poroids present on the copulae (Fig. 41).



FIGURES 33–42. *Fragilaria maarensis* sp. nov., SEM. 33, 34. Valve in external view displaying irregular spines at valve/mantle junction. 35. External view of central area showing ghost striae and rotae covered areolae. 36. Internal view of central area. 37. External view showing irregular orientation of marginal spines and fine groove at the site of the spines (arrow). 38, 40. External view of apex without rimoportula. Spines present. Apical pore field of ocellulimbus-type with 2–3 rows of poroids. 39. External view of apex with rimoportula and reduced apical pore field. 41. Internal view of apex without rimoportula. 42. Internal view of apex with rimoportula. Scale bar = 50 μm in Figs 33–34.

Type locality:—EL SALVADOR. Department of San Vicente: Lake Apastepeque, volcanic crater lake, 509 m a.s.l., 13°41'32.84"N, 88°44'42.41"W, sediment core sample (APA_D_28–30cm), 47 m water depth, collection: L. Macario-González and S. Cohuo-Durán, 09.10.2013. Holotype BR!: slide BR-4589 (Meise Botanic Garden, Belgium).

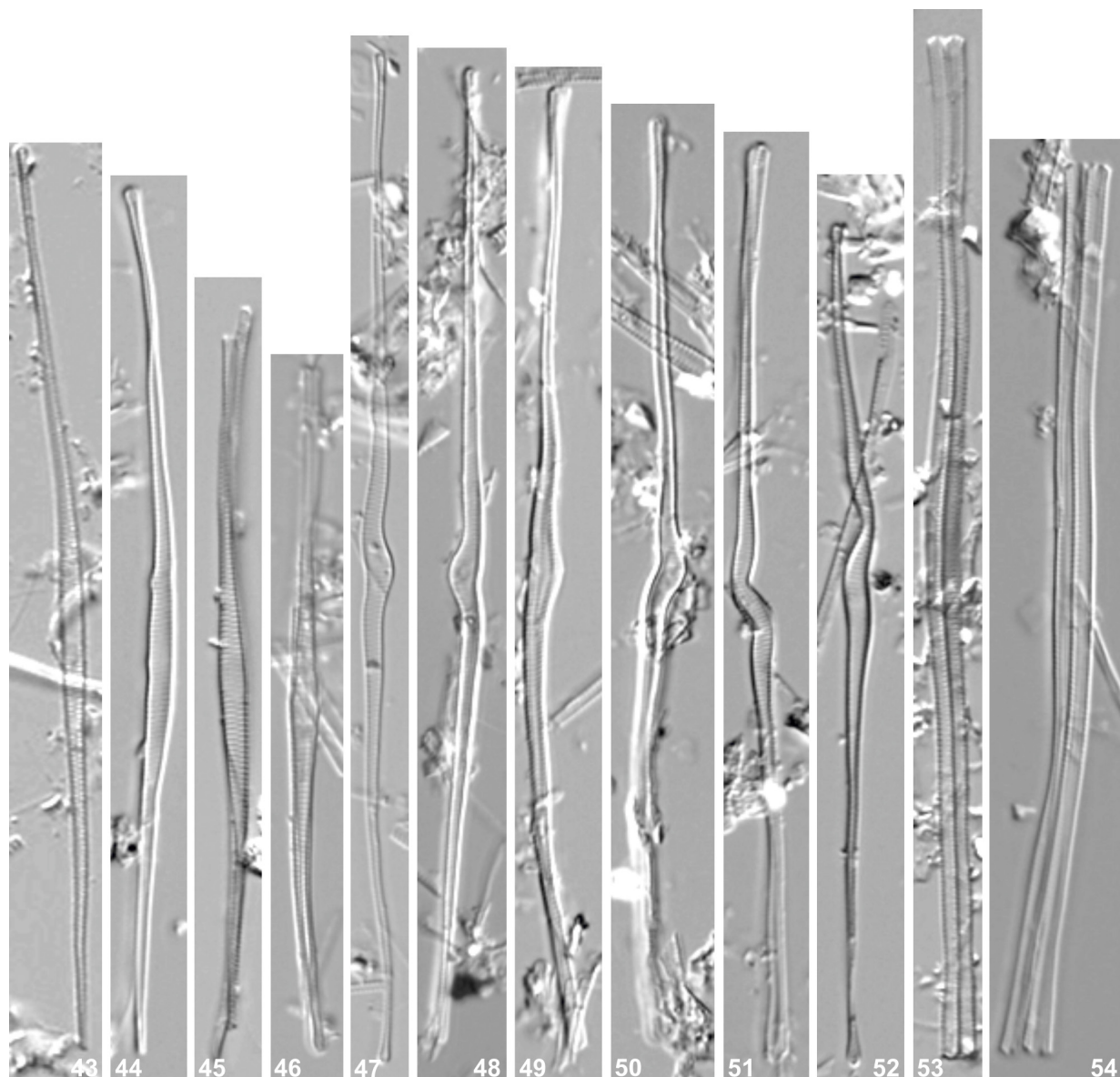
Etymology:—The specific epithet refers to the type of lake where the new species was found: maar lake.

Fragilaria huebeneri A.Schwarz, K.J.Krahn et C.E.Wetzel *sp. nov.*

(Figs 43–54 (LM), 55–65 (SEM))

Light microscope observations

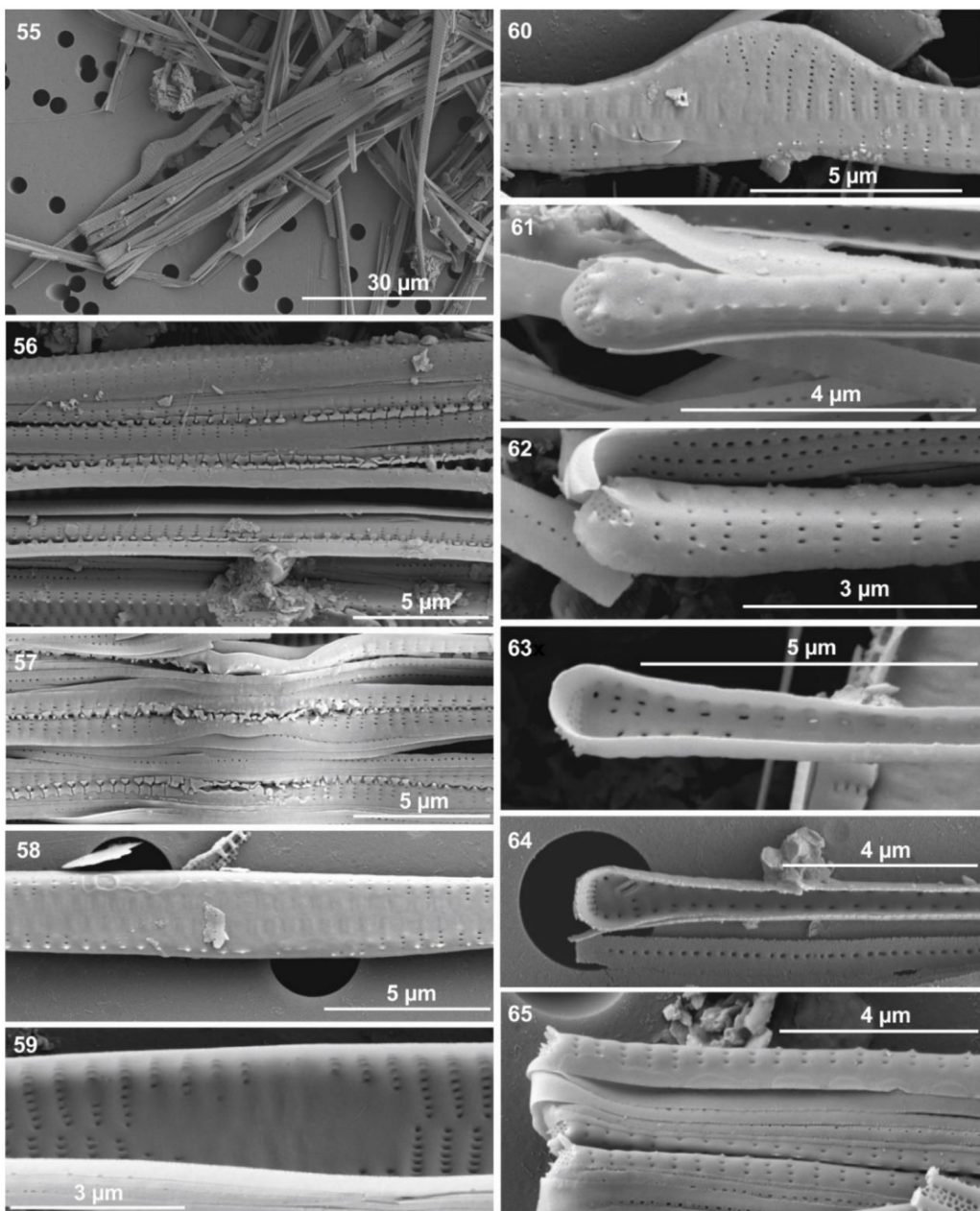
Cells living planktonic aggregated to ribbon-like colonies. Frustules narrowly rectangular in girdle view (Figs 53, 54). Valves spindle- to needle-shaped, narrowly lanceolate, tapering from a broadened center towards subcapitate apices, often curved and broken at the ends (Figs 43–46). Teratological forms frequently observed in the samples showing a sharp bend in the central part of the valve (Figs 47–52). Central area generally indistinct in LM, marked by ghost striae. Axial area narrow. Length 99–121 µm, width 2.0–2.9, becoming 0.5–0.9 µm subapically and 0.7–1.3 µm at the apices (n=35). Length-to-width ratio 39–52. Alternate striae, 17–21 in 10 µm. Teratological forms have slightly different dimensions, especially regarding their proximal width (n=10). Length 94–116 µm and width 1.7–3.2 µm. Width subapically 0.7–1.0, becoming 0.9–1.2 µm at the apices. Striae 19–21 in 10 µm.



FIGURES 43–54. *Fragilaria huebeneri* sp. nov., LM. 43–46. Straight forms. 47–52. Teratological forms. 53, 54. Girdle views. Scale bar = 10 µm.

Scanning electron microscope observations

Spatula-shaped spines on linking cells or small, irregular spines present in proximal part of valve located at junction between valve face and mantle, becoming reduced and absent towards the apices (Figs 55–58, 61, 62). Spines mostly located on vimines, sometimes near virgae (Fig. 56). Distinct, acute apical spines commonly observed (Figs 61, 62, 65). Areolae rounded (Figs 58, 59, 62, 65). Striae proximally composed of 2–5 rounded to elongated areolae on valve face and 2–4 areolae on mantle (Figs 56–59). Apical porefields of ocellulimbus-type with 3–5 rows of poroids. Central area is formed by absent and shortened striae (Figs 58–59). Central area of teratological forms often expanded on one side or bent, with deformed striae with numerous areolae (Fig. 60). One rimoportula is present per valve positioned at a distal end (Figs 62, 64). Plaques occasionally observed on the mantle (Fig. 65). Girdle bands open with a single row of small poroids on each copulae (Figs 56, 57, 65).



FIGURES 55–65. *Fragilaria huebeneri* sp. nov., SEM. 55. Overview image of sample showing straight and teratological forms. 56. Colony consisting of several frustules linked together by spatula-shaped spines. 57. Colony displaying central deformation. 58. External view of central area with ghost striae and small, acute spines. 59. Internal view of central area. 60. Central area of a teratological valve. 61. External view of apex without rimoportula. Small spines present. Apical pore field of ocellulimbus-type with five rows of poroids. 62. External view of apex with rimoportula and small spines surrounding the apical pore field. 63. Internal view of apex without rimoportula. 64. Internal view of apex with rimoportula. 65. Girdle view of apices.

Type locality:—TIBETAN PLATEAU (CHINA). Nam Co, subsaline lake, 4,730 m a.s.l., 30°40'00.0"N, 90°30'00.0"E, sediment trap sample (T2G2nd_30m), ~83 m water depth, collection: J. Wang *et al.*, May to September 2012. Holotype BR!: slide BR-4590 (Meise Botanic Garden, Belgium).

Etymology:—The specific epithet is named after an esteemed colleague and passionate diatomist – Thomas Hübener.

Results of morphometric and statistical analysis

Boxplots of the morphometric parameters valve length, valve width, stria density and length-to-width ratio clearly display the similarities and differences between *Fragilaria salvadoriana*, *F. maarensis*, and *F. huebeneri* (Fig. 66). In general, the length range of *F. salvadoriana* is wide and thus a less distinct feature (Fig. 66A). Although valves of *F. maarensis* are generally narrower than those of *F. salvadoriana* and *F. huebeneri*, values of the three species overlap and show comparable variability. Therefore, results suggest that the valve width is of less relevance for differentiation (Fig. 66B). The stria density of *F. salvadoriana*, however, is quite restricted and distinguishes this species from *F. maarensis* and *F. huebeneri* (Fig. 66C). The variability in valve length of the latter two is small and rarely overlaps. Therefore, this characteristic along with the length-to-width ratio appears suitable for distinguishing the two species (Figs 66A, D). Moreover, multivariate testing of the afore mentioned morphometric parameters (Fig. 67) shows highly significant differences between the three species (paired sample Hotelling's T-square test: $p < 0.001$).

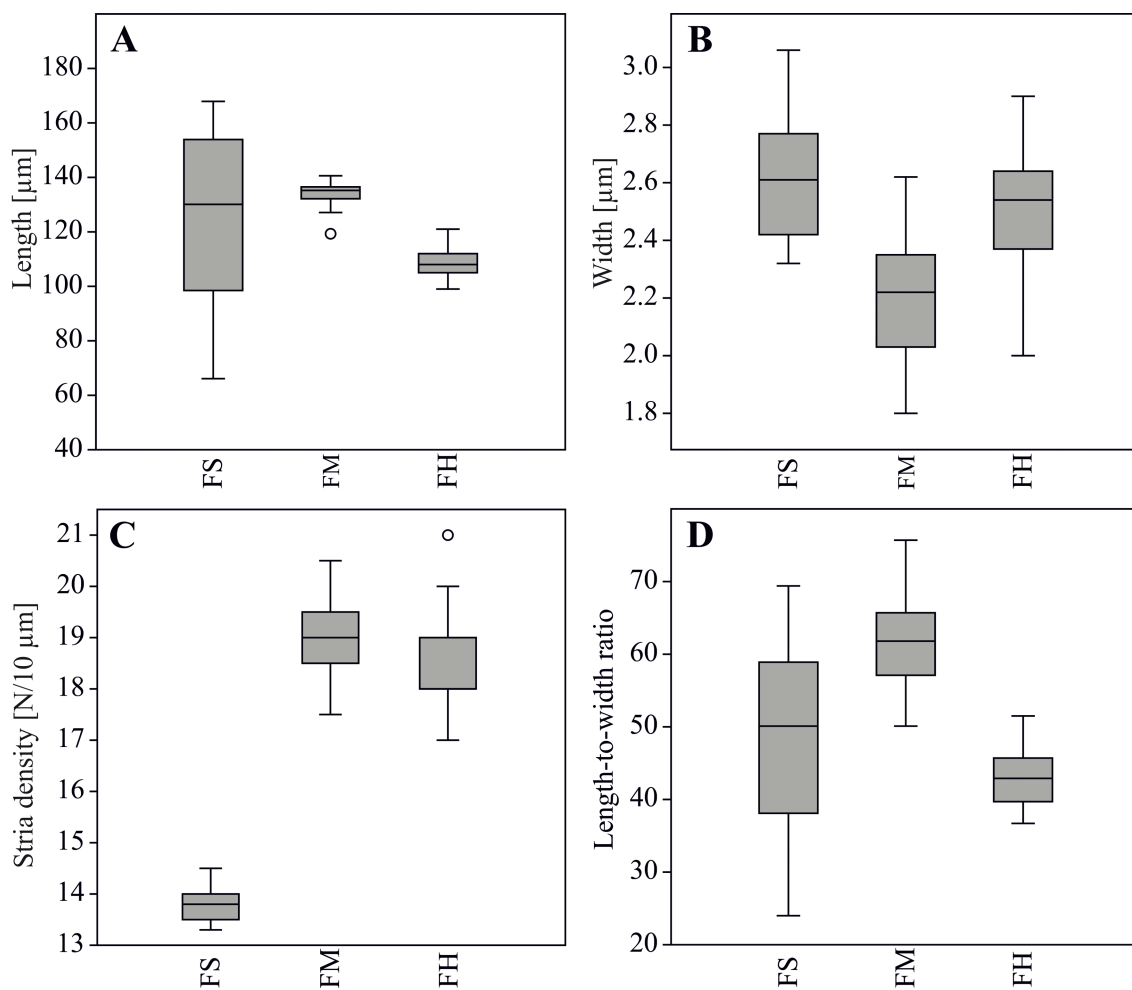


FIGURE 66. Box plots of morphological measurements of *Fragilaria salvadoriana* (FS), *F. maarensis* (FM), and *F. huebeneri* (n=35). A. Variability of valve length. B. Variability of valve width. C. Variability of stria density. D. Variability of the ratio length-to-width. For all boxplots, the median is shown with a horizontal line inside each box and boxes encompass the 25–75 percent quartiles. Whiskers are drawn from the maximum to the minimum value. If outliers are present, whiskers extend from the top/bottom of the box up to the largest/lowest data point less than 1.5 times the box height. Values outside the whisker range are shown as open circles.

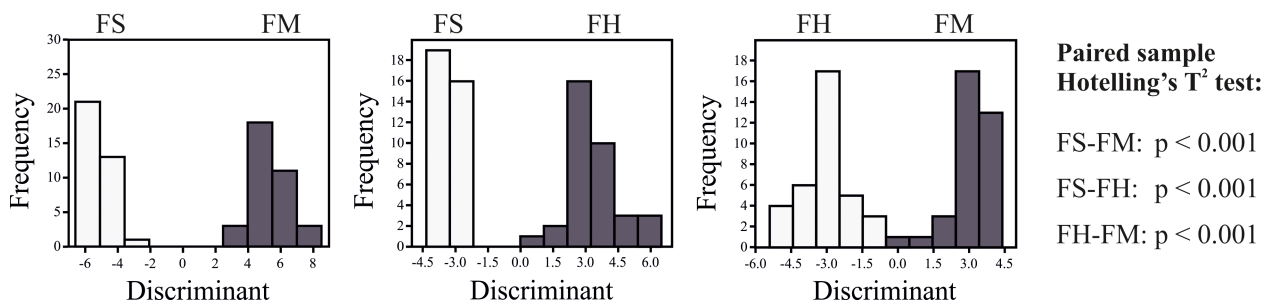


FIGURE 67. Hotelling's multivariate discriminant test histogram of *F. salvadorensis* (FS), *F. maarensis* (FM), and *F. huebeneri* (FH) and results of the paired sample Hotelling's T-square test.

Ecology and associated diatom flora

In modern sediments (surface sample, 0–1 cm) from Lake Apastepeque, *Fragilaria salvadorensis* and *F. maarensis* were only observed in small abundances (0.5% and 1.6%, respectively). However, in subfossil sediments, close to the bottom of the analyzed 30 cm core, the needle-shaped *Fragilaria* species were dominant (up to ~69% in total). Throughout the sediment core, especially *Achnanthidium neotropicum* Krahn & C.E.Wetzel in Krahn *et al.* (2018: 91) but also *Aulacoseira granulata* var. *granulata* (Ehrenberg 1843: 415) Simonsen (1979: 58), *A. granulata* var. *angustissima* (O.Müller 1899: 315) Simonsen (1979: 58), and *Ulnaria grunowii* (Lange-Bertalot & S.Ulrich 2014: 22) Cantonati et Lange-Bertalot in Kusber *et al.* (2017: 92) were abundantly found.

In October 2013 Lake Apastepeque had a relatively warm water temperature (29.5 °C), a low dissolved oxygen content (2.8 mg/L), an alkaline pH (8.6), and an electric conductivity of 100.0 µS/cm. Water analyses determined Ca²⁺ (17.9 mg/L, 0.89 meq/L) and Mg²⁺ (15.2 mg/L, 1.25 meq/L) to be the dominant cations, while HCO₃⁻ (145.2 mg/L, 2.38 meq/l) was the most important anion (Table 1). Therefore, *F. salvadorensis* and *F. maarensis* seem to occur in warm, magnesium-calcium-bicarbonate-rich freshwater lakes.

In all sequential and integral sediment trap samples from Nam Co covering the period from May 2012 to May 2013, *F. huebeneri* was abundant with an average relative abundance of 29.0% (n=29), and highest values of up to 81.7% in the summer. The type population of *F. huebeneri* was described from an integral sediment trap, installed from late May to mid-September 2012 at 30 m water depth. It dominated the assemblage (77.0%, thereof 23.2% teratological forms) and was accompanied predominantly by *Stephanodiscus transylvanicus* Pantocsek (1892: pl. 6: fig. 125) (8.3%), *Nitzschia subacicularis* Hustedt in A.Schmidt (1922: pl. 348: fig. 76) (3.5%), *Pantocsekiella ocellata* (Pantocsek 1901: 104) K.T.Kiss & Ács in Ács *et al.* (2016: 62) (2.6%), and *Amphora indistincta* Levkov (2009: 69) (2.3%).

Nam Co had a surface water temperature of 3.3–11.8 °C and dissolved oxygen content of 5.6–7.1 mg/L between May and September 2012 (Table 1). It was alkaline (9.4–9.9) and had an increased specific conductivity (1,716–1,851 µS/cm). Following the classification of Hammer (1986), Nam Co can be designated a subsaline lake. Dominant cation and anions of the lake water are Na⁺ (323.7 mg/L, 14.08 meq/L) and HCO₃⁻+CO₃²⁻ (1,111 mg/L), respectively. Considering the pH range, the dominant form of dissolved inorganic carbon (DIC) could be regarded as bicarbonate. Therefore, *F. huebeneri* appears to be characteristic for the plankton of alkaline, sodium-bicarbonate-dominated lakes with increased salinity.

Discussion and taxonomical remarks

The three new *Fragilaria* species described from El Salvador and the Tibetan Plateau are morphologically closely related to the needle-shaped species presented in Lange-Bertalot & Ulrich (2014). When only light microscopy is used, they might be difficult to distinguish from some other needle-shaped members of the genus due to overlaps in morphometric features.

Fragilaria salvadorensis can be clearly differentiated from *F. maarensis* and *F. huebeneri* by its lower stria density (Fig. 66C, Table 2). Furthermore, *F. salvadorensis* has a more linear-lanceolate valve outline, a dented, slightly constricted central area, and distinctly shaped marginal spines compared to the other two species. *Fragilaria maarensis* and *F. huebeneri* can mainly be distinguished by their length and length-to-width ratios (Figs 66A, 66D). Valves of *F. maarensis* have a lower number of areolae per stria (2–3, rarely 4) and less rows of poroids (2–3) at the apices than

F. huebeneri (3–5 and 3–5, respectively). One other characteristic feature of *F. huebeneri* is the formation of long, ribbon-like colonies linked together by spatula-shaped spines, which has not been observed in *F. salvadoraiana* and *F. maarensis*.

Fragilaria salvadoraiana

Fragilaria salvadoraiana resembles *F. crotonensis* ssp. *lacus-vulcani* Lange-Bertalot & S.Ulrich (2014: 43), *F. perdelicatissima* Lange-Bertalot & Van de Vijver in Lange-Bertalot & Ulrich (2014: 19), and *F. paludosa* (Meister 1912: 76) Lange-Bertalot & S.Ulrich (2014: 21) based on its rather coarse striae. However, valves of *F. crotonensis* ssp. *lacus-vulcani* are proximally inflated and never constricted. The central area is only indistinctly shaped by ghost striae in LM and in SEM, mostly acute spines can be observed.

Fragilaria perdelicatissima has a rather wide axial area, narrowly lanceolate valves, and a smaller apical (1.1–1.4 µm) and subapical (0.7–1.0 µm) width compared with *F. salvadoraiana* (1.3–1.7 µm and 1.0–1.5 µm, respectively). Especially in SEM, both taxa differ notably. While *F. salvadoraiana* has pronounced shark fin-shaped spines, marginal spines are absent on valves of *F. perdelicatissima*.

Fragilaria paludosa has wider valves (3.2–3.9 µm) and a smaller length-to-width ratio (22–29 instead of 24–65). The central area of *F. paludosa* is absent or indistinct, while valves of *F. salvadoraiana* have a distinctive, dented central area slightly constricted in appearance.

Taxa of the *F. tenera* (W.Smith 1856: 98) Lange-Bertalot (1980: 746) complex have a higher striae density and often more capitate apices. Spines are small pyramidal instead of shark fin-shaped. In contrast to *F. salvadoraiana*, *F. tenera* var. *tenera* has a sublinear to lanceolate valve outline and an indistinct central area in LM. *Fragilaria tenera* var. *lemanensis* J.C.Druart, S.Lavigne & M.Robert (2007: 284) can be differentiated by its formation of stellate colonies and higher apical width (1.4–2.5 µm). Valves of *F. tenera* var. *nanana* (Lange-Bertalot 1993: 48) Lange-Bertalot & S.Ulrich (2014: 7) are generally shorter (29–85 µm) and thinner (2.0–2.3 µm).

Fragilaria tenuissima Lange-Bertalot & S.Ulrich (2014: 15) differs from *F. salvadoraiana* in lower widths (proximal: 1.6–2.8 µm, apical: 0.7–1.0 µm, subapical: ≤1 µm) and higher stria density (16–20.5 in 10 µm). The striae of *F. tenuissima* are usually composed of four to seven areolae. This contrasts with *F. salvadoraiana*, which usually has two to five areolae per stria. Ultimately, valves of *F. tenuissima* have two rimoportulae, one on each apex, instead of one rimoportulae as observed on *F. salvadoraiana*, and spines are absent or reduced.

Fragilaria maarensis

Three new *Fragilaria* taxa with narrow, long valves and high stria density, which show some morphological similarities to *F. maarensis*, were recently described from tropical reservoirs in Brazil (Almeida *et al.* 2016, Wengrat *et al.* 2016). These are *F. billingsii* Wengrat, C.E.Wetzel & E.Morales in Wengrat *et al.* (2016: 196), *F. neotropica* P.D.Almeida, E.Morales & C.E.Wetzel in Almeida *et al.* (2016: 171) and *F. spectra* P.D.Almeida, E.Morales & C.E.Wetzel in Almeida *et al.* (2016: 174).

Fragilaria billingsii is significantly shorter (54–76 µm) than *F. maarensis* (119–141 µm) and has a lower length-to-width ratio (27–39). Moreover, its central area is bilaterally gibbous and the axial area lanceolate. Areolae of *F. maarensis* are occluded, which was not mentioned in the description of *F. billingsii*. With up to five areolae, the number of areolae per stria is higher on valves of *F. billingsii*.

Valves of *Fragilaria neotropica* are shorter (52–72 µm) and slightly thinner (1.7–2.0 µm), and show a higher stria density (28–32 in 10 µm) compared with *F. maarensis* (119–141 µm, 1.8–2.6 µm and 17.5–20.5/10 µm, respectively). Additionally, the species can be differentiated based on the capitate apices and inflated central area of *F. neotropica*. *Fragilaria spectra* differs from *F. maarensis* mostly in valve length (40.5–73.0 µm) and stria density (24–25 in 10 µm). Apices of *F. spectra* are acute to rounded and not subcapitate. In contrast to *F. maarensis*, valves of *F. spectra* do not develop marginal spines, have two rimoportulae, and up to five areolae per stria.

Fragilaria maarensis may be difficult to distinguish clearly from *F. saxoplanctonica* Lange-Bertalot & S.Ulrich (2014: 30). However, the latter has acutely rounded apices, the number of striae in 10 µm is higher (23–28), and the striae can be positioned opposing each other. Finally, *F. saxoplanctonica* lacks marginal spines and has proximally 5–6 areolae per stria.

There are strong similarities between *F. maarensis* and the *F. tenera* complex regarding stria density and width. Nonetheless, clear distinguishing features are the greater length, greater length-to-width ratio, differences in valve outline, and less capitate apices of *F. maarensis*.

TABLE 2. Comparison between *Fragilaria salvadorensis*, *F. maarensis* and *F. huebneri*, and the morphologically closest *Fragilaria* species (TF=teratol. forms).

	<i>Fragilaria salvadorensis</i> sp. nov.	<i>Fragilaria maarensis</i> sp. nov.	<i>Fragilaria huebneri</i> sp. nov.	<i>Fragilaria asiatica</i>	<i>Fragilaria asterionelloides</i>	<i>Fragilaria billingsii</i>	<i>Fragilaria crotensis</i>	<i>Fragilaria crotensis</i> ssp. <i>crotensis</i>	<i>Fragilaria cratonensis</i> ssp. <i>lacus-vulcani</i>
Colony formation	Loose aggregates observed	Loose aggregates observed	Ribbon-like	n.d.	Star-shaped	Not observed	Ribbon-shaped	At most few-celled, ribbon-shaped	
Valve length (μm)	66–168	119–141	99–121, TF: 94–116	31–102	60–70	54–76	40–170	55–120	
Valve width proximally (μm)	2.3–3.1	1.8–2.6	2.0–2.9, TF: 1.7–3.2	2–4	2	2.0–2.5	2–4(5), mostly 2.5–3.5	2.0–4.3	
Valve width subapically (μm)	1.0–1.5	0.7–1.3	0.5–0.9, TF: 0.7–1.0	n.d.	n.d.	n.d.	n.d.	0.7–1.5	
Valve width apically (μm)	1.3–1.7	1.0–1.7	0.7–1.3, TF: 0.9–1.2	n.d.	n.d.	n.d.	n.d.	1–2	
Length-to-width ratio	24–65	50–76	39–52	n.d.	n.d.	27–39	18–38 (and more)	18–49	
Valve outline	Narrowly linear-lanceolate	Very narrowly lanceolate	Spindle- to needle-shaped, narrowly lanceolate	Fusiform, becoming linear in larger valves	Lanceolate	Narrow, lanceolate	Narrowly lanceolate, proximal inflation, sometimes constricted	Narrowly lanceolate, proximal inflation, not constricted	
Striae in 10 μm	13.3–14.5	17.5–20.5	17–21, TF: 19–21	15–19	Subcapitate to slightly protracted	Capitate	17–20	15–18	
Apex	Subcapitate, rarely capitate	Subcapitate	Subcapitate	None, sometimes sternum widens to form an irregular central area	Expanded central area	Subcapitate	Weakly swollen	Capitate, subcapitate or simply rounded	
Central area	Distinct, appears dentate in LM, ghost striae	Distinct in LM, ghost striae	Often indistinct in LM, ghost striae	Often indistinct in LM, ghost striae	Expanded central area	Bilaterally gibbous	Rectangular, marked by ghost striae	Indistinctly shaped by ghost striae, sometimes unilateral, distinct in SEM	
Axial area	Narrow	Narrow to narrowly lanceolate	Narrow	Very narrow	Thin	Lanceolate	Very narrow	Very narrow	
Striation	Alternate	Alternate	Alternate	Opposite	Alternating	Alternating	Alternating	Alternating	
Areolae per side, proximally	2–5 on valve face, 2–4 on mantle	2–3, rarely 4 on valve face, 2–3 on mantle	3–5 on valve face, 2–4 on mantle	4–5	ca. 3–4	Up to 5	ca. 4	4–5	
Number of rimopulae	1	1	1	1	1–2	1	1	1	1
Apical pore field	Ocellulimbus-type, 2–4, rarely 5 rows of poroids	Ocellulimbus-type, 2–3 rows of poroids, sometimes reduced	Ocellulimbus-type, 3–5 rows of poroids	Small, externally: appears depressed, internally: ocellulimbi distinct	Ocellulimbus-type, three rows of poroids	Well developed, ocellulimbus-type	n.d.	n.d.	
Girdle bands	Open, single row of poroids on copulae	Open, single row of poroids on copulae	Open, single row of poroids on copulae	Single open copula, single row of poroids	Single open copula, single row of poroids	Open	Open	n.d.	n.d.
Spines	Shark fin-shaped	Acute, irregularly orientated, groove along the site	Proximally spatula-shaped or acute, reduced and absent towards the apices	Small spines, bifurcate at center	Angular to pyramidal	Proximally spatula-shaped, distally and on end cells of colonies short and acute	Mostly acute, sometimes spatula-shaped	Mostly acute, sometimes spatula-shaped	
Reference	This study	This study	This study	Rional <i>et al.</i> (2017)	Tuji & Williams (2017)	Wengert <i>et al.</i> (2016)	Lange-Bertalot & Ulrich (2014)	Lange-Bertalot & Ulrich (2014)continued on the next page

TABLE 2. (Continued)

	<i>Fragilaria neotropicica</i>	<i>Fragilaria perdelicatissima</i>	<i>Fragilaria paludosa</i>	<i>Fragilaria spectra</i>	<i>Fragilaria saxoplanconica</i>	<i>Fragilaria tenera</i> var. <i>lemanensis</i>	<i>Fragilaria tenera</i> var. <i>nana</i>	<i>Fragilaria tenera</i> var. <i>tenuissima</i>
Colony formation	Not observed	No colonies	n.d.	Not observed	No colonies	At most loose aggregates	Stellate colonies	No colonies
Valve length (μm)	52–72	36–95	73–110	40.5–73.0	40–170	60–120	70–80	29–85
Valve width proximally (μm)	1.7–2.0	2.0–2.6	3.2–3.9	1.5–2.5	1.8–2.5	2.0–3.5	2.0–2.3	1.6–2.8
Valve width subapically (μm)	n.d.	0.7–1.0	1.0–1.3	n.d.	0.6–0.85	0.8–1.0	0.8–1.1	0.7–1.0
Valve width apically (μm)	n.d.	1.1–1.4	1.3–1.8	n.d.	0.6–0.85	1.0–1.5	1.4–2.5	(0.5–0.75) 1.4–1.6 ≤1 (1–1.25)
Length-to-width ratio	n.d.	18–36	22–29	n.d.	22–59	27–49	29–37	13–29 38–72
Valve outline	Lanceolate, narrow, conspicuously inflated	Narrowly lanceolate	Linear-lanceolate	Linear-lanceolate	Very narrow fusiform to needle-shaped	Sublinear, lanceolate or slightly arcuate	Linear-lanceolate	Lanceolate Very narrowly lanceolate
Striae in 10 μm	28–32	14–17	13.9–15.3	24–25	23–28	18–20	16–19	18.5–20 16–20.5
Apex	Capitate, 2–3 spines, sometimes deflected	Subcapitate to capitate, no spines	Subcapitate	Acute to rounded	Acutely rounded, sometimes subapically weakly swollen	Capitate to subcapitate, 3–5 spines	Strongly capitate	Weakly subcapitate
Central area	Inflated, ghost striae, SEM: shortened striae	LM: ghost striae; SEM: distinct, limited by shortened striae	No central area or very indistinct	Rectangular, in SEM wide on both sides, no ghost striae	Indistinct in LM, ghost striae, in SEM rectangular	Absent	Distinct in LM, ghost striae, in SEM rectangular	Ghost striae, distinct in SEM
Axial area	Very narrow	Rather wide	Very narrow	Wider, lanceolate	Narrow, rather wide in LM	Narrow	Narrow	Narrow, linear
Striation	Alternate	Alternating	Alternating	Opposite or alternating	Alternating	Alternating	Alternating	Alternating
Areolae per side, proximally	1–3	n.d.	n.d.	Up to 5	5–6	n.d.	ca. 5	n.d. 4–7
Number of rimoportulae	1	1	n.d.	2	1	1	1	2
Apical pore field	Ocellulimbus-type, 2–3 rows of poroids	n.d.	n.d.	Ocellulimbus-type, 2–3 rows of poroids	Small, 2–3 rows of poroids	Ocellulimbus-type rows of poroids	Ocellulimbus-type rows of poroids	Ocellulimbus-type
Girdle bands	Open, with small, isolated perforations	n.d.	n.d.	Open	n.d.	Open, up to 3 copulae	n.d.	Open, with small, isolated perforations
Marginal spines	Small, pyramidal	Absent	n.d.	Absent	Absent	Small, pyramidal	Small, pyramidal	Small, reduced or absent
Reference	Almeida <i>et al.</i> (2016)	Lange-Bertalot & Ulrich (2014)	Almeida <i>et al.</i> (2016)	Lange-Bertalot & Ulrich (2014)	Druart <i>et al.</i> (2007), Lange-Bertalot & Ulrich (2014)	Lange-Bertalot & Ulrich (2014)	Lange-Bertalot & Ulrich (2014)	Lange-Bertalot & Ulrich (2014)

Fragilaria maarensis has a high potential to be misidentified as *F. tenuissima*. Both species overlap in length, width, and stria density and are morphologically close in valve outline and form of apices. However, the apical and subapical widths of *F. tenuissima* are generally smaller. Under the SEM, several differences are revealed. *F. tenuissima* possesses two rimoportulae per valve and the number of areolae per stria is notably higher (4–7 instead of 2–3, rarely 4).

Fragilaria huebeneri

As well as *F. huebeneri*, *F. asiatica* was described from the Tibetan Plateau. However, valves are smaller (31–102 µm) compared to *F. huebeneri* (99–121 µm) and have a fusiform to linear outline. In contrast to *F. huebeneri*, *F. asiatica* does not possess any spines and up to two rimoportulae can be present per valve. Furthermore, striae of *F. asiatica* are opposite instead of alternate.

Fragilaria asterionelloides Tuji & D.M.Williams (2017: 46) can be distinguished from *F. huebeneri* by the formation of star-shaped colonies and smaller size (60–70 µm). Apices of *F. asterionelloides* are more capitate and valves have a higher stria density of 22–23 per 10 µm. In SEM, bifurcate spines can be observed at the valve center of *F. asterionelloides*, whilst *F. huebeneri* rather develops spatula-shaped spines.

Regarding colony formation, *Fragilaria huebeneri* can be confused with *F. crotonensis* ssp. *crotonensis* Kitton (1869: 110). Both taxa form long ribbon-like colonies linked together by spatula-shaped spines. Otherwise, species have clear differentiating characteristics. *Fragilaria huebeneri* has a higher stria density (17–21 striae per 10 µm) than *F. crotonensis* ssp. *crotonensis* (15–18 striae per 10 µm), has a higher length-to-width ratio (39–52 to 18–38 and more, respectively) and shows no proximal constriction.

Fragilaria crotonensis ssp. *lacus-vulcani* forms only few-celled colonies and has generally lower stria density (14–18 striae per 10 µm) than *F. huebeneri*. The central area of *F. crotonensis* ssp. *lacus-vulcani* is distinct in LM, while it is often difficult to see in *F. huebeneri*.

Although found in a different geographical and climatic region, *F. huebeneri* is morphologically close to *F. neotropica*. The latter is mainly distinguished by shorter valves (52–72 µm), much higher stria density (28–32 in 10 µm), and capitate apices. Almeida *et al.* (2016) also described teratological forms in populations of *F. neotropica* from Brazilian reservoirs. Comparable to *F. huebeneri*, the valves show a central deformation. The authors suggest that deformation might be caused by metal contamination in the reservoirs.

Different types of environmental stressors have long been discussed as modifying valve morphology, including increased metal concentrations and trace elements (e.g. McFarland *et al.* 1997, Falasco *et al.* 2009, Cantonati *et al.* 2014, Lavoie *et al.* 2017). For example, the central deformation of valves of *F. tenera* (as *Synedra tenera* W. Smith) in Lake Orta, Italy have been ascribed to pollution by copper (Cu) (Ruggiu *et al.* 1998). In saline lakes on the Tibetan Plateau, extremely high levels of arsenic (As) were found. The accumulation is probably caused by natural loading and evaporation (Xiong *et al.* 2020). Soils on the Tibetan Plateau possess high natural As concentrations and in general, heavy metals mostly originate from weathering processes (Li *et al.* 2009, Sheng *et al.* 2012). Surface soil samples collected from the Lhasa–Shigatse–Nam Co region were found to be polluted with As, Cu, nickel (Ni), and mercury (Hg) to different degrees and may pose a potential ecological risk (Xie *et al.* 2014). Therefore, we propose that the deformation of the valves of *F. huebeneri* might be related to increased concentration of these elements in the lake water of Nam Co. However, further water analyses are needed to confirm this hypothesis.

A differentiation between *F. saxoplanctonica* and *F. huebeneri* can be made by the acutely rounded apices and the higher stria density (23–28 in 10 µm) of *F. saxoplanctonica*. Additionally, a central area and marginal spines are absent.

Fragilaria huebeneri resembles *F. tenera* var. *tenera* and the other two varieties. All taxa have a relatively similar stria density. However, *F. tenera* var. *tenera* forms loose aggregates at most, while *F. tenera* var. *lemanensis* forms stellate colonies, and no colony formation has been observed in *F. tenera* var. *nanana*. Valve lengths of *F. tenera* var. *lemanensis* and *F. tenera* var. *nanana* are smaller (70–80 µm and 29–85 µm, respectively) compared to *F. huebeneri* (99–121), whereas the length of *F. tenera* var. *tenera* is quite similar (60–120 µm). In contrast to *F. huebeneri*, *F. tenera* var. *tenera* has a more sublinear valve outline and apices of *F. tenera* var. *lemanensis* and *F. tenera* var. *nanana* are more capitate.

Fragilaria tenuissima is also difficult to distinguish from *F. huebeneri* in LM. Valve size, width, length-to-width ratio, and stria density largely overlap. *Fragilaria tenuissima*, however, does not form long colonies and apices are only weakly subcapitate. In SEM, two rimoportulae per valve are present in *F. tenuissima* instead of one in *F. huebeneri*, and spines are small or reduced. Moreover, *F. tenuissima* exhibits four to seven areolae per stria, whilst *F. huebeneri* has three to five areolae per stria.

Conclusion

The unique morphological characters of *Fragilaria salvadoriana*, *F. maarensis*, and *F. huebeneri* clearly distinguish these taxa from other species belonging to the needle-shaped *Fragilaria* group. While LM analyses are sufficient to limit the number of comparable species, especially features visible in SEM (e.g. spines, number of areolae per stria, and rimoportulae) allow definite differentiation. Valves of *F. salvadoriana* have a rather coarse striation and possess distinct shark fin-shaped spines. *Fragilaria maarensis* has very narrowly lanceolate valves, a high length-to-width ratio, and a relatively low number of areolae per stria. The combination of spatula-shaped linking spines, valve outline, stria density, and length-width-ratio distinguishes *F. huebeneri* from other similar taxa. Additionally, *F. huebeneri* was found in a subsaline lake, whereas most *Fragilaria* species occur in freshwater habitats. Although it has been argued that habitat preferences (freshwater vs. saline) should be considered when assigning a species to *Fragilaria*, other features attributed to this genus (open girdle bands, striae composed of single rows of areolae, one apical rimoportula, colony formation) support our allocation of *F. huebeneri*.

Fragilaria salvadoriana and *F. maarensis* were found in a warm, deep, and magnesium-calcium-bicarbonate-rich crater lake. The freshwater was characterized by an alkaline pH, low conductivity, and low dissolved oxygen content. *Fragilaria huebeneri* seems to prefer sodium-bicarbonate-rich waters. The species was abundant in the plankton of a large, deep, high elevation lake with an alkaline pH and increased specific conductivity.

So far, only few species of this genus have been described from the study areas. The continuing discovery of new *Fragilaria* taxa in recent years and the ongoing debate about the genus circumscription furthermore highlight the need for more taxonomical, ecological, and biogeographic studies to better understand boundaries and preferences. Moreover, well-founded taxonomic analyses prior to ecological interpretations are fundamental for reliable environmental inferences and evaluation. Detailed microscopic investigation together with a comprehensive ecological assessment and, if possible, molecular analysis form the basis for applied fields such as biomonitoring and paleolimnology and should be further pursued.

Acknowledgements

We would like to thank the following colleagues and institutions that made sampling in Lake Apastepeque, El Salvador possible: Eleonor de Tott, Roberto Moreno (Universidad del Valle de Guatemala, Guatemala); Consejo Nacional de Áreas Protegidas (CONAP, Guatemala); Néstor Herrera (Ministerio de Medio Ambiente, San Salvador), and the students Lisa Heise, Cuauhtémoc Ruiz, and Ramón Beltrán. The limnological survey in El Salvador was financially supported by the Deutsche Forschungsgemeinschaft (DFG) via grant Schw 671/16-1. CONACYT (Mexico) gave fellowships (218604, 218639) to S. Cohuo and L. Macario. Nam Co project funding was granted by the National Natural Science Foundation of China (Grant No. 41877168) and CADY project (TP2:03G0813F) from Bundesministerium für Bildung und Forschung (BMBF), Germany. We thank the anonymous reviewer for the constructive and critical comments that helped to improve the manuscript. The authors would like to thank Jinlei Kai for providing data from Nam Co. Part of the funding for this research was also provided in the framework of the DIATOMS project (LIST - Luxembourg Institute of Science and Technology).

References

- Ács, E., Ari, E., Duleba, M., Dressler, M., Genkal, S.I., Jakó, E., Rimet, F., Ector, L. & Kiss, K.T. (2016) *Pantocsekiella*, a new centric diatom genus based on morphological and genetic studies. *Fottea, Olomouc* 16: 56–78.
<https://doi.org/10.5507/fot.2015.028>
- Almeida, P.D., Morales, E.A., Wetzel, C.E., Ector, L. & Bicudo, D.C. (2016) Two new diatoms in the genus *Fragilaria* Lyngbye (Fragilariothyceae) from tropical reservoirs in Brazil and comparison with type material of *F. tenera*. *Phytotaxa* 246: 163–183.
<https://doi.org/10.11646/phytotaxa.246.3.1>
- Alcocer, J., Lugo, A., Escobar, E., Sanchez, M.R. & Vilaclara, G. (2000) Water column stratification and its implications in the tropical warm monomictic Lake Alchichica, Puebla, Mexico. *Verhandlungen des Internationalen Verein Limnologie* 27: 3166–3169.
<https://doi.org/10.1080/03680770.1998.11898262>

- Anslan, S., Azizi Rad, M., Buckel, J., Echeverria Galindo, P., Kai, J., Kang, W., Keys, L., Maurischat, P., Nieberding, F., Reinosch, E., Tang, H., Tran, T.V., Wang, Y. & Schwalb, A. (2020) Reviews and syntheses: How do abiotic and biotic processes respond to climatic variations in the Nam Co catchment (Tibetan Plateau)? *Biogeosciences* 17: 1261–1279.
<https://doi.org/10.5194/bg-17-1261-2020>
- Armenteras, D., Gibbes, C., Vivacqua, C., Espinosa, J., Duleba, W., Goncalves, F. & Castro, C. (2016) Interactions between Climate, Land Use and Vegetation Fire Occurrences in El Salvador. *Atmosphere* 7: 26.
<https://doi.org/10.3390/atmos7020026>
- Battarbee, R.W., Jones, V.J., Flower, R.J., Cameron, N.G., Bennion, H., Carvalho, L. & Juggins, S. (2001) Diatoms. In: Smol, J.P., Birks, H.J.B. & Last, W.M. (Eds.) *Tracking Environmental Change Using Lake Sediments. Volume 3: Terrestrial, Algal, and Siliceous Indicators*. Kluwer Academic Publishers, Dordrecht, 155–202.
<https://doi.org/10.1007/0-306-47668-1>
- Bloesch, J. & Burns, N.M. (1980) A critical review of sedimentation trap technique. *Schweizerische Zeitschrift für Hydrologie* 42: 15–55.
<https://doi.org/10.1007/BF02502505>
- Cantonati, M., Angeli, N., Virtanen, L., Wojtal, A.Z., Gabrieli, J., Falasco, E., Lavoie, I., Morin, S., Marchetto, A., Fortin, C. & Smirnova, S. (2014) *Achnanthidium minutissimum* (Bacillariophyta) valve deformities as indicators of metal enrichment in diverse widely-distributed freshwater habitats. *Science of the Total Environment* 475: 201–215.
<https://doi.org/10.1016/j.scitotenv.2013.10.018>
- Castillejo, P., Chamorro, S., Paz, L., Heinrich, C., Carrillo, I., Salazar, J.G., Navarro, J.C. & Lobo, E.A. (2018) Response of epilithic diatom communities to environmental gradients along an Ecuadorian Andean River. *Comptes Rendus Biologies* 341: 256–263.
<https://doi.org/10.1016/j.crvi.2018.03.008>
- Céspedes-Vargas, E., Umaña-Villalobos, G. & Silva-Benavides, A.M. (2016) Tolerancia de diez especies de diatomeas (Bacillariophyceae) a los factores fisico-químicos del agua en Río Sarapiquí, Costa Rica. *Revista de Biología Tropical* 64: 105–115.
<https://doi.org/10.15517/rbt.v64i1.18295>
- Chudaev, D.A. & Georgiev, A.A. (2016) New taxa of *Navicula* sensu stricto (Bacillariophyta, Naviculaceae) from high-altitude lake in Tibet, China. *Phytotaxa* 243: 180–184.
<https://doi.org/10.11646/phytotaxa.243.2.9>
- Druart, J.C., Lavigne, S. & Robert, M. (2007) *Fragilaria tenera* var. *lemanensis*, une nouvelle variété pour le Léman (France-Suisse). *Cryptogamie Algologie* 28: 283–287.
- Ehrenberg, C.G. (1843) Mittheilungen über 2 neue asiatische Lager fossiler Infusorien-Erden aus dem russischen Trans-Kaukasien (Grusien) und Sibirien. *Bericht über die zur Bekanntmachung geeigneten Verhandlungen der Königlich-Preussischen Akademie der Wissenschaften zu Berlin* 1843: 43–49.
- Falasco, E., Bona, F., Badino, G., Hoffmann, L. & Ector, L. (2009) Diatom teratological forms and environmental alterations: a review. *Hydrobiologia* 623: 1–35.
<https://doi.org/10.1007/s10750-008-9687-3>
- Flores-Stulzer, E., Villalobos-Sandí, N., Piedra-Castro, L. & Scholz, C. (2017) Evaluación breve de la presencia de diatomeas y su relación con algunos parámetros físico-químicos en el río Pirro, Heredia, Costa Rica. *Uniciencia* 31: 99–109.
<https://doi.org/10.15359/ru.31-2.7>
- Gasse, F., Fontes, J.C., van Campo, E. & Wie, K. (1996) Holocene environmental changes in Bangong Co basin (Western Tibet). Part 4: Discussions and conclusions. *Palaeogeography, Palaeoclimatology, Palaeoecology* 120: 79–92.
[https://doi.org/10.1016/0031-0182\(95\)00035-6](https://doi.org/10.1016/0031-0182(95)00035-6)
- Gou, P., Ye, Q., Che, T., Feng, Q., Ding, B., Lin, C. & Zong, J. (2017) Lake ice phenology of Nam Co, Central Tibetan Plateau, China, derived from multiple MODIS data products. *Journal of Great Lakes Research* 43: 989–998.
<https://doi.org/10.1016/j.jglr.2017.08.011>
- Haberyan, K.A., Horn, S.P. & Cumming, B.F. (1997) Diatom assemblages from Costa Rican lakes: an initial ecological assessment. *Journal of Paleolimnology* 17: 263–274.
<https://doi.org/10.1023/A:1007933130319>
- Hammer, Ø., Harper, D.A.T. & Ryan, P.D. (2001) Past: Paleontological Statistics Software Package for Education and Data Analysis. *Palaeontologica Electronica* 4: 1–9.
- Hammer, U.T. (1986) *Saline Lake Ecosystems of the World*. Monographiae Biologicae 59. Dr. W. Junk Publishers, Dordrecht, 616 pp.
- Hotelling, H. (1951) A generalized T test and measure of multivariate dispersion. – In: Newman, J. (Ed.) *Proceedings of the second Berkeley Symposium on Mathematical Statistics and Probability*, University of California Press, Berkeley: 23–42.
- Huang, C. (1979) *The Quaternary diatoms of Yangtzejengensis, Tibet*. Contribution to the Geology of the Qing Hai-Xizang (Tibet) Plateau, 176–195.

- Hustedt, F. (1922) *Bacillariales aus Innerasien. Gesammelt von Dr. Sven Hedin*. In: Hedin, S. (Ed.) *Southern Tibet, discoveries in former times compared with my own researches in 1906–1908*. Stockholm, Lithographic Institute of the General Staff of the Swedish Army 6: 107–152.
<https://doi.org/10.5962/bhl.title.64226>
- Hustedt, F. (1953) La flora de diatomeas en paredones sobrehumedecidos en El Salvador. *Comunicaciones del Instituto Tropical de Investigaciones Científicas de la Universidad de El Salvador* 2: 129–138.
- Jao, C.-C. (1964) Some freshwater algae from southern Tibet. *Oceanologia et Limnologia Sinica* 6: 169–189.
- Jao, C.-C., Zhu, H.Z. & Lee, Y.Y. (1974) The fresh-water algae from Mount Qomolangma district (in Tibet). Report of the Scientific Survey of Mount Qomolangma District, 1966–1968: 92–126.
- Jiménez, I., Sánchez-Mármol, L. & Herrera, N. (2004) Inventario Nacional y Diagnóstico de los humedales de El Salvador. MARN/AECI. Sal Salvador, El Salvador C.A.
- Kahlert, M., Kelly, M.G., Mann, D.G., Rimet, F., Sato, S., Bouchez, A. & Keck, F. (2019) Connecting the morphological and molecular species concepts to facilitate species identification within the genus *Fragilaria* (Bacillariophyta). *Journal of Phycology* 55: 948–970.
<https://doi.org/10.1111/jpy.12886>
- Kai, J., Wang, J., Ju, J., Huang, L., Ma, Q., Daut, G. & Zhu, L. (2020) Spatio-temporal variations of hydrochemistry and modern sedimentation processes in the Nam Co basin, Tibetan Plateau: Implications for carbonate precipitation. *Journal of Great Lakes Research* 46: 961–975.
<https://doi.org/10.1016/j.jglr.2020.04.006>
- Kitton, F. (1869) Notes on New York diatoms with description of a new species *Fragilaria crotonensis*. *Hardwicke's Science-Gossip* 5: 109–110.
- Kociolek, J.P., You, Q., Liu, Q., Liu, Y. & Wang, Q. (2020) Continental diatom biodiversity discovery and description in China: 1848 through 2019. *PhytoKeys* 160: 45–97.
<https://doi.org/10.3897/phytokeys.160.54193>
- Krahn, K.J., Wetzel, C.E., Ector, L. & Schwalb, A. (2018) *Achnanthidium neotropicum* sp. nov., a new freshwater diatom from Lake Apastepeque in El Salvador (Central America). *Phytotaxa* 382: 89–101.
<https://doi.org/10.11646/phytotaxa.382.1.4>
- Kusber, W.-H., Cantonati, M. & Lange-Bertalot, H. (2017) Validation of five diatom novelties published in “Freshwater Benthic Diatoms of Central Europe” and taxonomic treatment of the neglected species *Tryblionella hantzschiana*. *Phytotaxa* 328: 90–94.
<https://doi.org/10.11646/phytotaxa.328.1.6>
- Lange-Bertalot, H. (1980) Zur systematischen Bewertung der bandförmigen Kolonien bei *Navicula* und *Fragilaria*. Kriterien für die Vereinigung von *Synedra* (subgen. *Synedra*) Ehrenberg mit *Fragilaria* Lyngbye. *Nova Hedwigia* 33: 723–787.
- Lange-Bertalot, H. (1993) 85 neue Taxa und über 100 weitere neu definierte Taxa ergänzend zur Süßwasserflora von Mitteleuropa, Vol. 2/1–4. *Bibliotheca Diatomologica* 27: 1–164.
- Lange-Bertalot, H. & Metzeltin, D. (2009) A dystrophic mountain lake in Panama - Hot spot of new and rare neotropical diatoms. *Nova Hedwigia* 135: 137–165.
- Lange-Bertalot, H. & Ulrich, S. (2014) Contributions to the taxonomy of needle-shaped *Fragilaria* and *Ulnaria* species. *Lauterbornia* 78: 1–73.
- Lavoie, I., Hamilton, P.B., Morin, S., Kim Tiam, S., Kahlert, M., Gonçalves, S., Falasco, E., Fortin, C., Gontero, B., Heudre, D., Kojadinovic-Sirinelli, M., Manoylov, K., Pandey, L.K. & Taylor, J.C. (2017) Diatom teratologies as biomarkers of contamination: Are all deformities ecologically meaningful?. *Ecological Indicators* 82: 539–550.
<https://doi.org/10.1016/j.ecolind.2017.06.048>
- Lazhu, Y.K., Wang, J., Lei, Y., Chen, Y., Zhu, L., Ding, B. & Qin, J. (2016) Quantifying evaporation and its decadal change for Lake Nam Co, central Tibetan Plateau. *Journal of Geophysical Research: Atmospheres* 121: 7578–7591.
<https://doi.org/10.1002/2015JD024523>
- Levkov, Z. (2009) *Amphora* sensu lato. In: Lange-Bertalot (Ed.) *Diatoms of Europe: Diatoms of the European Inland Waters and Comparable Habitats*. Vol. 5. Ruggell: A.R.G. Gantner Verlag K.G., pp. 5–916.
- Li, C., Kang, S. & Zhang, Q. (2009) Elemental composition of Tibetan plateau top soils and its effect on evaluating atmospheric pollution transport. *Environmental Pollution* 157: 2261–2265.
<https://doi.org/10.1016/j.envpol.2009.03.035>
- Li, J.Y. (1983) The diatom fossils from Diatomaceous Earth of Sipangul Lake, Region Xizang. In: *Contribution to the Geology of Qinghai-Xizang (Tibet) Plateau*. Vol. 4. Geological Publishing House, Beijing, pp. 272–319.
- Li, Y.L., Williams, D., Metzeltin, D., Kociolek, J.P. & Gong, Z.J. (2010) *Tibetiella pulchra* gen. nov. et sp. nov., a new freshwater epilithic diatom (Bacillariophyta) from River Nujiang in Tibet, China. *Journal of Phycology* 46: 325–330.

- https://doi.org/10.1111/j.1529-8817.2009.00776.x
- Liu, Q., Yang, L., Nan, F., Feng, J., Lv, J., Kociolek, J.P. & Xie, S. (2018) A new diatom species of *Aneumastus* D. G. Mann & Stickle (Bacillariophyta, Bacillariophyceae, Mastogloiales, Mastogloaceae) from Tibet, China. *Phytotaxa* 373: 231–235.
<https://doi.org/10.11646/phytotaxa.373.3.6>
- Liu, Q., Li, J., Nan, F., Feng, J., Lv, J., Xie, S. & Kociolek, J.P. (2019) New and interesting diatoms from Tibet: I. Description of a new species of *Clipeoparvus* Woodbridge et al. *Diatom Research* 34: 33–38.
<https://doi.org/10.1080/0269249X.2019.1578697>
- Lyngbye, H.C. (1819) *Tentamen hydrophytologiae danicae continens omnia hydrophyta cryptogama Daniae, Holsatiae, Faeroae, Islandiae, Groenlandiae hucusque cognita, systematicae disposita, descripta et iconibus illustrata, adjectis simul speciebus norvegicis.* Hafniae, Copenhagen, Denmark, 248 pp, 70 pls.
<https://doi.org/10.5962/bhl.title.6079>
- McFarland, B.H., Hill, B.H. & Willingham, W.T. (1997) Abnormal *Fragilaria* spp. (Bacillariophyceae) in streams impacted by mine drainage. *Journal of Freshwater Ecology* 12: 141–149.
<https://doi.org/10.1080/02705060.1997.9663517>
- MARN (Ministerio de Medio Ambiente y Recursos Naturales) (2015) *Boletín Climatológico Mensual*, Anual 2015, 16 pp.
- Medlin, L., Jung, I., Bahulikar, R., Mendgen, K., Kroth, P. & Kooistra, W.H.C.F (2008) Evolution of the diatoms. VI. Assessment of the new genera in the araphids using molecular data. *Nova Hedwigia, Beiheft* 133: 81–100.
- Meister, F. (1912) *Die Kieselalgen der Schweiz. Beiträge zur Kryptogamenflora der Schweiz. Matériaux pour la flore cryptogamique suisse.* Vol. IV, fasc. 1. Bern: Druck und Verlag von K.J. Wyss, pp. [i]–vi, [1]–254, 48 pls.
- Mereschkowsky, C. (1906) Diatomées du Tibet. *Imperial Russkoe geograficheskoe obshchestvo* 8: 1–40.
- Meyer-Abich, H. & Williams, H. (1956) The Apastepeque Volcanic Field. *Anales del Servicio Geológico Nacional de El Salvador* 2: 62–67.
- Michels, A. (1998a) Use of diatoms (Bacillariophyceae) for water quality assessment in two tropical streams in Costa Rica. *Revista de Biología Tropical* 46, Supplement 6: 143–152.
- Michels, A. (1998b) Effects of sewage water on diatoms (Bacillariophyceae) and water quality in two tropical streams in Costa Rica. *Revista de Biología Tropical* 46, Supplement 6: 153–175.
- Michels, A., Umaña, G. & Raeder, U. (2006) Epilithic diatom assemblages in rivers draining into Golfo Dulce (Costa Rica) and their relationship to water chemistry, habitat characteristics and land use. *Archiv für Hydrobiologie* 165: 167–190.
<https://doi.org/10.1127/0003-9136/2006/0165-0167>
- Michels-Estrada, A. (2003) Ökologie und Verbreitung von Kieselalgen in Fließgewässern Costa Ricas als Grundlage für eine biologische Gewässergütebeurteilung in den Tropen. *Dissertationes Botanicae* 377: 1–244.
- Mittelbach, G.G., Schemske, D.W., Cornell, H.V., Allen, A.P., Brown, J.M., Bush, M.B., Harrison, S.P., Hurlbert, A.H., Knowlton, N., Lessios, H.A., McCain, C.M., McCune, A.R., McDade, L.A., McPeek, M.A., Near, T.J., Price, T.D., Ricklefs, R.E., Roy, K., Sax, D.F., Schlüter, D., Sobel, J.M. & Turelli, M. (2007) Evolution and the latitudinal diversity gradient: speciation, extinction and biogeography. *Ecology Letters* 10 (4): 315–331.
<https://doi.org/10.1111/j.1461-0248.2007.01020.x>
- Morales, E.A. (2003) *Fragilaria pennsylvanica*, a new diatom (Bacillariophyceae) species from North America, with comments on the taxonomy of the genus *Synedra* Ehrenberg. *Proceedings of the Academy of Natural Sciences of Philadelphia* 153: 155–166.
[https://doi.org/10.1635/0097-3157\(2003\)153\[0155:FPANDB\]2.0.CO;2](https://doi.org/10.1635/0097-3157(2003)153[0155:FPANDB]2.0.CO;2)
- Morales, E.A., Wetzel, C.E., Rivera, S.F., Van de Vijver, B. & Ector, L. (2014) Current taxonomic studies on the diatom flora (Bacillariophyceae) of the Bolivian Altiplano, South America, with possible consequences for palaeoecological assessments. *Journal of Micropalaeontology* 33: 121–129.
<https://doi.org/10.1144/jmpaleo2014-007>
- Müller, O. (1899) Bacillariaceen aus den Natronthälern von El Kab (Ober-Aegypten). *Hedwigia* 38: 274–288, 289–321, pls 10–12.
- Paillès, C., Sylvestre, F., Escobar, J., Tonetto, A., Rustig, S. & Mazur, J.C. (2018) *Cyclotella petenensis* and *Cyclotella cassandrae*, two new fossil diatoms from Pleistocene sediments of Lake Petén-Itzá, Guatemala, Central America. *Phytotaxa* 351: 247–263.
<https://doi.org/10.11646/phytotaxa.351.4.1>
- Pantocsek, J. (1892) *Beiträge zur Kenntnis der Fossilen Bacillarien Ungarns. Teil III: Süßwasser Bacillarien. Anhang-analysen 15 neuer Depots von Bulgarien, Japan, Mahern, Russland und Ungarn.* Nagytapolcsány Topo, Buchdruckerei von Julius Platzko, pls. 42.
- Pantocsek, J. (1901) *Die Kieselalgen oder Bacillarien des Balaton. Im Auftrage der ungarischen geographischen Gesellschaft auf Basis eigener Aufsammlungen. In: Resultate der wissenschaftlichen Erforschung des Balatonsees.* II. Band. Anhang zur II. Section des 2. Theiles. K. und K. Hofbuchdruckerei des Victor Hornyánszky, Budapest, 112 pp.
<https://doi.org/10.5962/bhl.title.64368>
- Pérez, L., Lorenschat, J., Massaferro, J., Paillès, C., Sylvestre, F., Hollwedel, W., Brandorff, G.O., Brenner, M., Islebe, G., Lozano, M.S.,

- Scharf, B. & Schwalb, A. (2013) Bioindicators of climate and trophic state in lowland and highland aquatic ecosystems of the Northern Neotropics. *Revista de Biología Tropical* 61: 603–644.
<https://doi.org/10.15517/rbt.v61i2.11164>
- Patrick, R.M. & Reimer, C.W. (1966) The Diatoms of the United States exclusive of Alaska and Hawaii, Vol. I: Fragilariaeae, Eunotiaceae, Achanthaceae, Naviculaceae. *Monographs of the Academy of Natural Sciences of Philadelphia* 13: 1–688.
<https://doi.org/10.2307/1351135>
- Rioual, P., Flower, R.J., Chu, G., Lu, Y., Zhang, Z., Zhu, B. & Yang, X. (2017) Observations on a fragilaroid diatom found in inter-dune lakes of the Badain Jaran Desert (Inner Mongolia, China), with a discussion on the newly erected genus *Williamsella* Graeff, Kociolek & Rushforth. *Phytotaxa* 329: 28–50.
<https://doi.org/10.11646/phytotaxa.329.1.2>
- Round, F.E., Crawford, R.M. & Mann, D.G. (1990) *The Diatoms. Biology and morphology of the genera*. Cambridge University Press, Cambridge, U.K., 747 pp.
- Ruggiu, D., Luglié, A., Cattaneo, A. & Panzani, P. (1998) Paleoecological evidence for diatom response to metal pollution in Lake Orta (N. Italy). *Journal of Paleolimnology* 20: 333–345.
<https://doi.org/10.1023/A:1007929926526>
- Rühland, K., Paterson, A.M. & Smol, J. (2015) Diatom assemblage responses to warming: Reviewing the evidence. *Journal of Paleolimnology* 54: 1–35.
<https://doi.org/10.1007/s10933-015-9837-3>
- Sayre, A.N. & Taylor, G.C., Jr. (1951) Ground-water resources of the Republic of El Salvador, Central America. *Geological Survey Water Supply Paper* 1079-D: 155–255.
<https://doi.org/10.3133/wsp1079D>
- Schmidt, A. (1922) *Atlas der Diatomaceenkunde*. Heft 87. Reisland, Leipzig, pls 345–348.
- Schwalb, A., Steeb, P., Wrozyne, C., Mäusbacher, R., Daut, G., Wallner, J., Kroemer, E., Gleixner, G., Muegler, I., Sachse, D., Mosbrugger, V. & Schütt, B. (2008) The top of the world as a climate sensor. *German Research* 30: 4–7.
<https://doi.org/10.1002/geom.200890029>
- Sheng, J.J., Wang, X.P., Gong, P., Tian, L.D. & Yao, T.D. (2012) Heavy metals of the Tibetan top soils. *Environmental Science and Pollution Research* 19: 3362–3370.
<https://doi.org/10.1007/s11356-012-0857-5>
- Silva-Benavides, A.-M. (1996a) The epilithic diatom flora of a pristine and a polluted river in Costa Rica, Central America. *Diatom Research* 11: 105–142.
<https://doi.org/10.1080/0269249X.1996.9705368>
- Silva-Benavides, A.-M. (1996b) The use of water chemistry and benthic diatom communities for qualification of a polluted tropical river in Costa Rica. *Revista de Biología Tropical* 44: 395–416.
- Simonsen, R. (1979) The diatom system: ideas on phylogeny. *Bacillaria* 2: 9–71.
- Skvortzow, B.V. (1935) Diatomées récoltées par le Père E. Licent au cours de ses voyages dans le Nord de la Chine au bas Tibet, en Mongolie et en Mandjourie. *Publications du Musée Hoangho Paiho de Tien Tsin* 36: 1–43.
- Smith, W. (1856) *A synopsis of the British Diatomaceae; with remarks on their structure, functions and distribution; and instructions for collecting and preserving specimens*, Vol. 2. John van Voorst, London, 107 pp., pls 32–60, 61–62, A–E.
<https://doi.org/10.5962/bhl.title.10706>
- Tuji, A. & Williams, D.M. (2017) *Fragilaria asterionelloides*, a new planktonic species of *Fragilaria* from Japanese reservoirs that forms star-shaped colonies. *Bulletin of the National Museum of Natural Science, series B* 43: 45–50.
- Van Campo, E. & Gasse, F. (1993) Pollen-and diatom-inferred climatic and hydrological changes in Sumxi Co basin (western Tibet) since 13,000 yr B.P. *Quaternary Research* 39: 300–313.
<https://doi.org/10.1006/qres.1993.1037>
- Vázquez, G., Favila, M.E., Madrigal, R., Del Olmo, C.M., Baltanás, A. & Bravo, M.A. (2004) Limnology of crater lakes in Los Tuxtlas, Mexico. *Hydrobiologia* 523: 59–70.
<https://doi.org/10.1023/B:HYDR.0000033095.47028.51>
- Wang, J., Zhu, L., Daut, G., Ju, J., Lin, X., Wang, Y. & Zhen, X. (2009) Investigation of bathymetry and water quality of Lake Nam Co, the largest lake on the central Tibetan Plateau, China. *Limnology* 10: 149–158.
<https://doi.org/10.1007/s10201-009-0266-8>
- Wang, J., Zhu, L., Wang, Y., Ju, J., Xie, M. & Daut, G. (2010) Comparisons between the chemical compositions of lake water, inflowing river water, and the lake sediment in Nam Co, central Tibetan Plateau, China and their controlling mechanisms. *Journal of Great Lakes Research* 36: 587–595.
<https://doi.org/10.1016/j.jglr.2010.06.013>

- Wang, J., Huang, L., Ju, J., Daut, G., Wang, Y., Ma, Q., Zhu, L., Haberzettl, T., Baade, J. & Mausbacher, R. (2019) Spatial and temporal variations in water temperature in a high-altitude deep dimictic mountain lake (Nam Co), central Tibetan Plateau. *Journal of Great Lakes Research* 45: 212–223.
<https://doi.org/10.1016/j.jglr.2018.12.005>
- Wang, J., Huang, L., Ju, J., Daut, G., Ma, Q., Zhu, L., Haberzettl, T., Baade, J., Mäusbacher, R., Hamilton, A., Graves, K., Olsthoorn, J. & Laval, B. (2020) Seasonal stratification of a deep, high-altitude, dimictic lake: Nam Co, Tibetan Plateau. *Journal of Hydrology* 584: 124668.
<https://doi.org/10.1016/j.jhydrol.2020.124668>
- Wengrat, S., Morales, E.A., Wetzel, C.E., Almeida, P.D., Ector, L. & Bicudo, D.C. (2016) Taxonomy and ecology of *Fragilaria billingsii* sp. nov. and analysis of type material of *Synedra rumpens* var. *fusa* (Fragilariaeae, Bacillariophyta) from Brazil. *Phytotaxa* 270: 191–202.
<https://doi.org/10.11646/phytotaxa.270.3.3>
- Wetzel, C.E. & Ector, L. (2014) *Planothidium lagerheimii* comb. nov. (Bacillariophyta, Achnanthales) a forgotten diatom from South America. *Phytotaxa* 188: 261–267.
<https://doi.org/10.11646/phytotaxa.188.5.3>
- Williams, D.M. (2011) *Synedra, Ulnaria*: definitions and descriptions – a partial resolution. *Diatom Research* 26: 149–153.
<https://doi.org/10.1080/0269249X.2011.587646>
- Williams, D.M. (2019) Spines and homologues in ‘araphid’ diatoms. *Plant Ecology and Evolution* 152 (2): 150–162.
<https://doi.org/10.5091/plecevo.2019.1597>
- Williams, D.M. & Round, F.E. (1986) Revision of the genus *Synedra* Ehrenb. *Diatom Research* 1: 313–339.
<https://doi.org/10.1080/0269249X.1986.9704976>
- Williams, D.M. & Round, F.E. (1987) Revision of the genus *Fragilaria*. *Diatom Research* 2: 267–288.
<https://doi.org/10.1080/0269249X.1987.9705004>
- Williams, H. & Meyer-Abich, H. (1955) Volcanism in the southern part of El Salvador with particular reference to the collapse basins of Lakes Coatepeque and Ilopango. *University California Publications in Geol Sci* 32: 1–64.
- Witkowski, W., Lange-Bertalot, H. & Metzeltin, D. (2000) *Diatom flora of marine coasts I*. In: Lange-Bertalot, H. (Ed.) *Iconographia Diatomologica, Vol. 7*. A.R.G. Gantner Verlag K.G., Ruggell, Liechtenstein. 925 pp.
- Wydrzycka, U. & Lange-Bertalot, H. (2001) Las diatomeas (Bacillariophyceae) acidófilas del río Agrio y sitios vinculados con su cuenca, volcán Poás, Costa Rica. *Brenesia* 55–56: 1–68.
- Xie, H., Li, J., Zhang, C., Tian, Z., Liu, X., Tang, C., Han, Y. & Liu, W. (2014) Assessment of Heavy Metal Contents in Surface Soil in the Lhasa–Shigatse–Nam Co Area of the Tibetan Plateau, China. *Bulletin of Environmental Contamination and Toxicology* 93: 192–198.
<https://doi.org/10.1007/s00128-014-1288-4>
- Xiong, X., Zhang, K., Chen, Y., Qu, C. & Wu, C. (2020) Arsenic in water, sediment, and fish of lakes from the Central Tibetan Plateau. *Journal of Geochemical Exploration* 210: 106454.
<https://doi.org/10.1016/j.gexplo.2019.106454>
- Yang, X., Wang, S., Xia, W. & Li, W. (2001) Application of CCA for study on modern lake diatoms and environment in the Tibetan Plateau. *Science in China Series D-Earth Sciences* 44: 343.
<https://doi.org/10.1007/BF02912005>
- Yang, X., Kamenik, C., Schmidt, R. & Wang, S. (2003) Diatom-based conductivity and water-level inference models from eastern Tibetan (Qinghai-Xizang) Plateau lakes. *Journal of Paleolimnology* 30: 1–19.
<https://doi.org/10.1023/A:1024703012475>
- Yu, S., Wang, J., Li, Y., Peng, P., Kai, J., Kou, Q. & Laug, A. (2019) Spatial distribution of diatom assemblages in the surface sediments of Selin Co, central Tibetan Plateau, China, and the controlling factors. *Journal of Great Lakes Research* 45: 1069–1079.
<https://doi.org/10.1016/j.jglr.2019.09.006>
- Zhang, G., Yao, T., Xie, H., Zhang, K. & Zhu, F. (2014) Lakes’ state and abundance across the Tibetan Plateau. *Chinese Science Bulletin* 59: 3010–3021.
<https://doi.org/10.1007/s11434-014-0258-x>
- Zhu, H.Z. & Chen, J.Y. (1995) New taxa of Diatom (Bacillariophyta) from Xizang (Tibet) I. *Acta Phytotaxonomica Sinica* 33: 516–519.
- Zhu, H.Z. & Chen, J.Y. (1996) New taxa of Diatom (Bacillariophyta) from Xizang (Tibet) II. *Acta Phytotaxonomica Sinica* 34: 102–104.